Gondwana Research 35 (2016) 164–179

Contents lists available at ScienceDirect

Gondwana Research

journal homepage: www.elsevier.com/locate/gr

Source region analyses of the morainal detritus from the Grove Mountains: Evidence from the subglacial geology of the Ediacaran–Cambrian Prydz Belt of East Antarctica

Jianmin Hu [a,b,*], Minghua Ren [c], Yue Zhao [a,b], Xiaochun Liu [a,b], Hong Chen [a,b]

[a] Institute of Geomechanics, Chinese Academy of Geosciences, Beijing 100081, China
[b] Key Laboratory of Paleomagnetism and Tectonic Reconstruction of Ministry of Land and Resources, China
[c] Department of Geoscience, University of Nevada Las Vegas, NV 89154, USA

ARTICLE INFO

Article history:
Received 7 July 2014
Received in revised form 24 April 2015
Accepted 24 April 2015
Available online 23 May 2015

Handling Editor: J.G. Meert

Keywords:
Antarctica
Grove Mountains
Detrital zircon
U–Pb dating
Subglacial geology
High-pressure granulite

ABSTRACT

The Grove Mountains are the inland exposures of the Prydz Belt in East Antarctica. Although the 550–500 Ma orogenic event was recognized as the latest major magmatic–metamorphic activity in the Prydz Belt, its subduction–collision origin was not confirmed until the discovery of high-pressure (HP) mafic granulite erratic boulders in the glacial moraines from the Grove Mountains. Because no HP metamorphic bedrock is exposed in this area, an understanding the regional geology required a thorough study of the morainal debris mineralogy and detrital zircon U–Pb chronology. Detrital zircon U–Pb age histograms show 550–450 Ma, 900–800 Ma, and 1100–1000 Ma modes from three morainal deposits and one paleosol samples. The oldest ages were 2300 to 2420 Ma. Detailed electron probe microanalyses (EPMA) for the detrital mineral grains were compared with the minerals from the nearby exposed bedrock. The mineral chemistry indicates that the exposed bedrock in the Grove Mountains was not the sole source for morainal materials. This new U–Pb zircon geochronology and microprobe mineral data support the previous interpretation that the 550–500 Ma tectonic activity was the final collisional event that formed the Prydz Belt and amalgamated East Antarctica.

1. Introduction

The East Antarctic continent is part of the Gondwana supercontinent and is comprised of several Archean–Paleoproterozoic cratons (Black et al., 1986; Fanning et al., 1995; Harley and Black, 1997; Oliver and Fanning, 1997; Peucat et al., 1999; Oliver and Fanning, 2002) and Proterozoic–Paleozoic orogenic belts (Tingey, 1991; Kinny et al., 1993; Flöttmann and Oliver, 1994; Chen et al., 1995; Meert and Van Der Voo, 1997; Harley et al., 1998; Fitzsimons, 2000a; Powell and Pisarevsky, 2002; Meert, 2003; Boger and Miller, 2004; Kelsey et al., 2008; Meert and Lieberman, 2008; Boger, 2011; Harley et al., 2013). Previous studies suggested that East Antarctica formed from several fragments during Neoproterozoic to Cambrian time (Black et al., 1992; Shiraishi et al., 1992; Dirks and Wilson, 1995; Hensen and Zhou, 1995; Jacobs et al., 1995; Sheraton et al., 1995; Hensen and Zhou, 1997; Motoyoshi and Ishikawa, 1997; Fitzsimons, 2000a; Fraser et al., 2000; Powell and Pisarevsky, 2002; Meert, 2003; Shiraishi et al., 2003; Boger and Miller, 2004; Meert and Lieberman, 2008; Boger, 2011; Godard and Palmeri, 2013; Harley et al., 2013; Meert, 2014). The margins of stable continental blocks evolved in multiple stages and the orogenic belts contain complicated late Meso–early Neoproterozoic (Grenvillian) to Neoproterozoic–Cambrian (Pan-African) overlapping frameworks during cyclical continental evolutions (Fitzsimons, 2000a; Meert, 2003; Veevers, 2004; Will et al., 2009, 2010; Godard and Palmeri, 2013; Meert, 2014). The term Pan-African has been used to describe Neoproterozoic to early Paleozoic (870–550 Ma) protracted tectonic, magmatic, and metamorphic activities covering a wide range of spatial scales within Gondwana (Kröner, 1984; Stern, 1994; Kröner and Stern, 2004). The 550–500 Ma tectonism along the margins of Antarctica, southern India and into the Zambezi and Damara Belts were named the Kuunga Orogeny (Meert et al., 1995; Meert and Van Der Voo, 1997; Meert, 2003). Within the mobile belts, the high-pressure (HP) metamorphic rocks are the critical indicators revealing the collisional continental boundaries (Di Vincenzo et al., 1997; Di Vincenzo and Palmeri, 2001; Board et al., 2005; Palmeri et al., 2007; Liu et al., 2009b; Romer et al., 2009; Godard and Palmeri, 2013). East Antarctic HP rocks are mostly buried under the large ice sheets and are rarely exposed (Godard and Palmeri, 2013), so any evidence of HP metamorphic rocks in this part of Antarctica is worthy of attention. Based on the timing of tectonic activity and the presence of HP metamorphic rocks in outcrop and glacial deposits, the Prydz Belt and Lützow Holm Belt was identified as the loci of suture zones that assembled East Antarctica from three continental fragments (Dirks and Wilson, 1995; Hensen and Zhou, 1997; Fitzsimons,

* Corresponding author at: Institute of Geomechanics, Chinese Academy of Geosciences, Beijing 100081, China.

http://dx.doi.org/10.1016/j.gr.2015.04.010
1342-937X/

2000a; Zhao et al., 2000; Boger et al., 2001; Fitzsimons, 2003; Harley, 2003; Meert, 2003; Zhao et al., 2003; Liu et al., 2006, 2007a, 2009a,b; Harley et al., 2013).

The Prydz Belt is Ediacaran–Cambrian age mobile belt extending from Prydz Bay to the Gamburstsev Subglacial Mountains (Fitzsimons, 2000a; Zhao et al., 2003; Liu et al., 2006, 2009a,b). The Grove Mountains are located about 400 km inland from Prydz Bay in line with the Prydz Belt and are composed of isolated nunataks (Fig. 1). Adjacent to nunatak exposures in the central Grove Mountains, irregular morainal deposits form elongated bands distributed on the ice sheet (Fig. 2). The morainal detritus originated by rock fragments accumulating by the weathering of the nearby cliffs and material excavated from the bedrock under the ice cap during the movement of glaciers.

The glacial deposits are important in the study of Antarctic geology because of limited bedrock exposures, especially for the inland parts of the Antarctic continent (Di Vincenzo et al., 1997; Peucat et al., 2002; Di Vincenzo et al., 2007; Elliot and Fanning, 2008; Veevers et al., 2008; Veevers and Saeed, 2013; Elliot et al., 2015). The morainal deposits from the edge of the glaciers and the inland continental ice sheet usually carry considerable information about the subglacial bedrock (Jenkins and Alibert, 1991; Goodge et al., 2004; Jamieson et al., 2005; Veevers and Saeed, 2008; Goodge and Fanning, 2010; Veevers and Saeed, 2011, 2013). The 542 to 545 Ma HP metamorphosed mafic granulites, which are the fundamental evidence of the subduction–collision feature of the Prydz Belt, were collected from the morainal boulders at the Gale Escarpment, Grove Mountains (Liu et al., 2009a). The HP granulite bedrock exposures have not yet been found. Therefore, locating the source of the high-pressure metamorphosed mafic granulites required that our study focus on morainal deposits from different glacial valleys to analyze the detrital mineral assemblages and the detrital zircon U–Pb geochronology. The chemical character of detrital minerals from the Grove Mountains was compared with the mineral chemistry of the local and regional bedrock to identify the source regions of the morainal deposits. This morainal gravel study has provided additional evidence for the metamorphic processes of the Prydz Belt and the evolution of East Antarctica.

2. Regional context and previous study of the Grove Mountains

2.1. Regional context

East Antarctica, part of eastern Gondwana, experienced multiple orogenic events. Several subduction–collision events sutured Archean–Paleoproterozoic terranes during both the late Mesoproterozoic to early

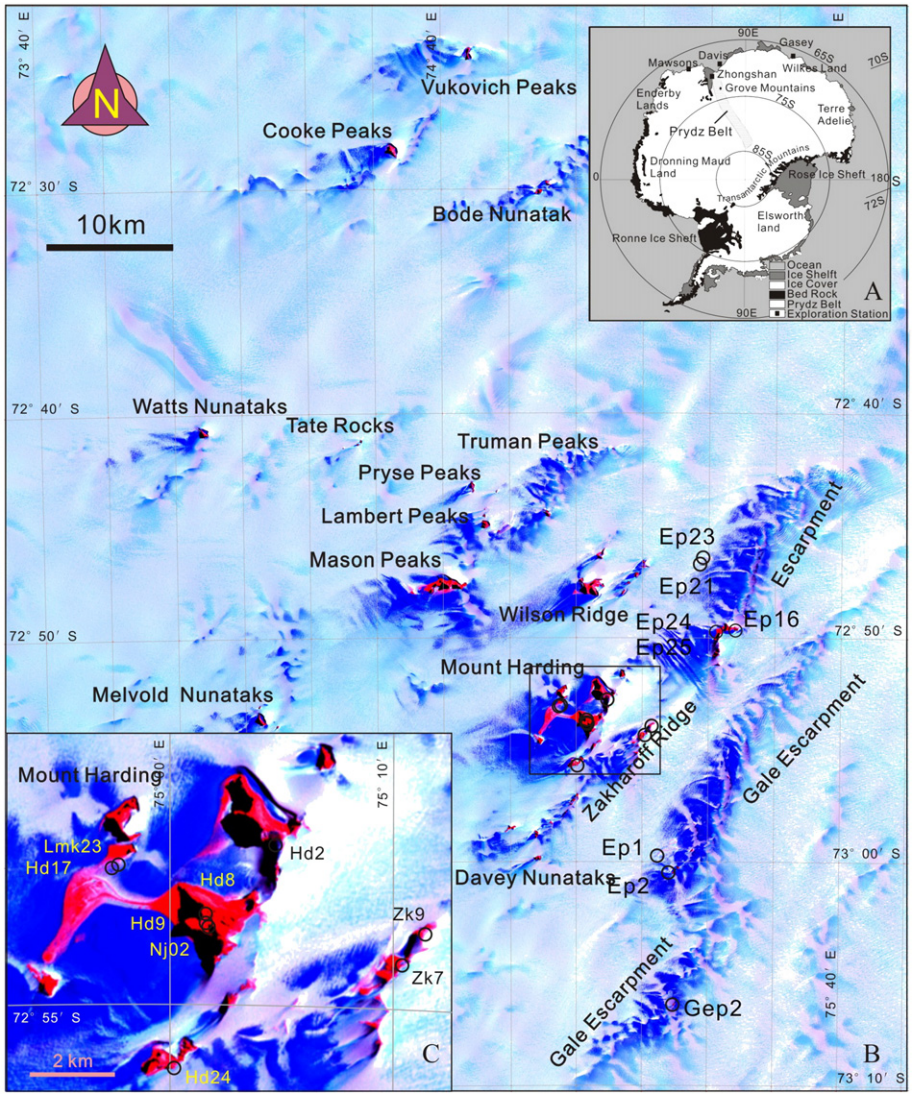

Fig. 1. Remote sensing image of the Grove Mountains, Antarctica. This image includes three parts: A) the upper right corner shows the bedrock distribution in Antarctica and the locations of the Grove Mountains and Prydz Belt, B) the center remote sensing image is the Grove Mountains area, showing the locations of all the nunataks and the sample locations at Gale Escarpment, C) the lower left corner shows the Mount Harding area and the sample locations.

Fig. 2. Gravel belts in the Grove Mountains. a. #1 morainal belt to the west of south Gale Escarpment; b. #2 morainal belt to the west of north Gale Escarpment; c. morainal belt to the west of Mount Harding, d. large boulders in the gravel belt at the foot of west Mount Harding.

Neoproterozoic orogenies (Grenvillian) (Lovering et al., 1981; Tingey, 1982; Sheraton et al., 1984; Harley, 1987; Fitzsimons and Harley, 1991; Hoffman, 1991; Moores, 1991; Tingey, 1991; Kinny et al., 1993; White and Clarke, 1993; Fanning et al., 1995; Paul et al., 1995; Kinny et al., 1997; Daly et al., 1998; Boger et al., 2000; Fitzsimons, 2000b, 2003; Wang et al., 2008; Halpin et al., 2012; Meert, 2014) and the late Neoproterozoic to early Paleozoic orogenic event (Zhao et al., 1992; Shiraishi et al., 1994; Hensen and Zhou, 1995; Meert et al., 1995; Carson et al., 1996; Fitzsimons et al., 1997; Meert and Van Der Voo, 1997; Boger et al., 2000; Meert, 2003; Boger et al., 2006; Santosh et al., 2006; Wang et al., 2007; Wilson et al., 2007; Meert and Lieberman, 2008; Rino et al., 2008; Veevers and Saeed, 2008; Boger, 2011; Godard

Table 1
Summary of zircon U–Pb ages near Grove Mountains area.

Location	Area	Age (Ma)	Method	Rock type	References
Grove Mountains	Gale Escarpment	2582 ± 9, 531 ± 14	SHRIMP	Charnockite	Liu et al. (2009a)
	Bryse Peaks	2052 ± 4, 475 ± 29	LA-ICPMS	Paragneiss	Liu et al. (2007a)
	Zakharoff Ridge	1907 ± 26, 907 ± 21 545 ± 9	SHRIMP	Mafic Granulite	
	Mason Peaks	742 ± 18, 549 ± 8	SHRIMP	two pyroxenes granulite	
	Melvold Nunataks	910, 529 ± 14	SHRIMP	Orthogneiss	Zhao et al. (2000)
	Mason Peaks	914 ± 17, 536 ± 8	SHRIMP	Orthogneiss	Liu et al. (2007a)
	Zakharoff Ridge	922 ± 32, 535 ± 5	TIMS	Orthogneiss	
	Mount Harding	910 ± 14, 544 ± 5	LA-ICPMS	Orthogneiss	
	Melvold Nunataks	548 ± 9	SHRIMP	two pyroxenes granulite	
	Wilson Mountain	501 ± 7	TIMS	Granite	Zhao et al. (2000)
	Mount Harding	547 ± 1	SHRIMP	Charnockite	Liu et al. (2006)
	Gale Escarpment	545 ± 6, 542 ± 6	SHRIMP	Charnockite	Liu et al. (2009a)
	Davey Nunataks	503 ± 2	SHRIMP	Layered granite	Liu et al. (2006)
Rauer Island	Scherbinina Island	3470 + 30, 528 + 12	SHRIMP	Tonalitic gneiss	Harley et al. (1998)
	Torckler Island	3267 ± 17, 498 ± 28	SHRIMP	Paragneiss	Kinny et al. (1993)
	Scherbinina Island	2844 ± 6, 512 ± 12	SHRIMP	Garnet-Oxide–Quartz vein	Harley et al. (1998)
	Short Point	2801 ± 6, 540 ± 19	SHRIMP	Felsic orthogneiss	Kinny et al. (1993)
	Filla Island	1027 ± 59, 515 ± 58	SHRIMP	Felsic orthogneiss	
	Hop Island	1000 ± 51, 490 ± 90	SHRIMP	Felsic orthogneiss	
	Macey Peninsula	511 ± 6	SHRIMP	Gneiss	Sims et al. (2001)
	Scherbinina Island	511 ± 10	SHRIMP	Fe-amphibolite	Harley et al. (1998)
Southwest Prydz Bay	Larsemann Hills	1106 ± 11, 535 ± 7	SHRIMP	Quartzite	Zhao et al. (1995)
	Larsemann Hills	~1100	SHRIMP	Orthogneiss	Wang et al. (2003)
	Larsemann Hills	~990	SHRIMP	Charnockite	
	Brattstrand Bluffs	535 ± 13, 518 ± 3	SHRIMP	Light color gneiss	Fitzsimons et al. (1997)
	Bolingen Islands	527 ± 14	SHRIMP	Felsic granite	Hand and Kinny (1996)
	Larsemann Hills	516 ± 7, 514 ± 7	SHRIMP	Granite	Carson et al. (1996)
	Landing Bluffs	500 ± 4	SHRIMP	Granite	Tingey (1991)
Amery Ice Shelf	Vestfold Hills	2526–2475		Gneiss, mafic granulite	Black et al. (1991)
	McKaskle Hills	1019 ± 33, 545 ± 15	SHRIMP	Garnet granulite	Liu et al. (2007b)
	McKaskle Hills	1137 ± 46	SHRIMP	Two pyroxene granulite	
	McKaskle Hills	932 ± 15, 533 ± 10	SHRIMP	Paragneiss	
	McKaskle Hills	1174 ± 26, 529 ± 11	SHRIMP	Orthogneiss	

and Palmeri, 2013). New and more precise geochronology helped identify the late Neoproterozoic to early Paleozoic tectonothermal event (550–500 Ma) within the Grenville mobile belt at Prydz Bay (Zhao et al., 1991, 1992; Dirks and Wilson, 1995; Carson et al., 1996), Denman Glacier (Black et al., 1992; Sheraton et al., 1995), Lützow–Holm Bay (Shiraishi et al., 1992, 1994; Motoyoshi and Ishikawa, 1997; Fraser et al., 2000) and central Dronning Maud Land (Jacobs et al., 1995; Shiraishi et al., 2003). With the recognition of those Ediacaran–Cambrian tectonothermal events at the Joinet Seoul Island and the Grove Mountains (Zhao et al., 2000; Liu et al., 2003; Zhao et al., 2003; Liu et al., 2007a, 2009a,b), the Prydz Belt was identified as a tectonic suture zone transecting the inland of East Antarctica (Fitzsimons, 2000a; Liu et al., 2002; Meert, 2003; Zhao et al., 2003; Liu et al., 2006, 2009a,b).

In order to better understand the timing of geological events in the Prydz Belt region, U–Pb zircon isotopic ages are compiled in Table 1.

In the Vestfold Hill area, the Archean–Paleoproterozoic shield is composed of 2526–2475 Ma mafic granulite, felsic orthogneiss, and paragneiss (Oliver et al., 1982; Black et al., 1991; Snape et al., 1997). A large number of Paleo-Mesoproterozoic period (2470–1241 Ma) mafic dike swarms (mainly diabase) also crop out in the area (Lanyon et al., 1993; Seitz, 1994; Bain et al., 2001).

In the Rauer Islands, an Archean tonalitic gneiss complex was emplaced in two stages at 3470–3270 and 2850–2800 Ma respectively (Kinny et al., 1993; Harley et al., 1998). The Mesoproterozoic mafic and felsic intrusions were formed at 1060–1000 Ma (Kinny et al., 1993; Harley et al., 1998; Sims et al., 2001; Tong et al., 2002; Harley, 2003) and the monazite from paragneiss was dated at 948 ± 12 Ma (Kelsey et al., 2007). These dates are suggestive of a Grenvillian metamorphic event. During the Ediacaran–Cambrian period, all units experienced high-grade metamorphism. Zircon U–Pb ages, garnet and whole rock Sm–Nd isochrons, and monazite U–Th–Pb ages for orthogneiss, paragneiss, mafic granulite, and granitic pegmatite all recorded this 530 to 490 Ma activity (Fitzsimons et al., 1997; Hensen and Zhou, 1997; J.X. Zhao et al., 1997; Y. Zhao et al., 1997; Harley et al., 1998; Sims et al., 2001; Zhao et al., 2001, 2003; Kelsey et al., 2003a, 2007; Wang et al., 2003; Wilson et al., 2007). Additionally, a monazite U–Th–Pb date from the high-grade metapelite is 511 Ma and falls in the same age range as the others (Kelsey et al., 2003b).

From the Larsemann Hills near Prydz Bay, the zircon core age for quartzite is 1100 Ma (Zhang et al., 1996), similar to 1200 to 1100 Ma detrital zircon ages recorded for other samples in the area (Zhao et al., 1995). Amphibole and biotite $^{40}Ar/^{39}Ar$ isochron ages are 514 to 486 Ma for gneiss, granite, and pegmatite (Zhao et al., 1992, 1993; Hensen and Zhou, 1995; Y. Zhao et al., 1997). Zircon rim U–Pb ages for quartzite (Zhao et al., 1991, 1992, 1993; Zhang et al., 1996), orthogneiss, and mafic granulites (Wang et al., 2003) range from 541 to 528 Ma. Granite and granulite ages are 516 to 500 Ma based on garnet and whole rock Sm–Nd isochrones and a whole rock Rb–Sr isochron (Tingey, 1991; Zhao et al., 1992, 1993; Thost et al., 1994; Hensen and Zhou, 1995; Carson et al., 1996).

Zircon U–Pb and monazite U–Th–Pb ages for gneiss from Brattstrand Bluffs are 535 to 527 Ma and 518 to 512 Ma (Zhao et al., 1992; Hand and Kinny, 1996; Fitzsimons et al., 1997). The monazite U–Th–Pb ages are 915 to 864 Ma for the paragneiss in the Bolingen Islands (Kelsey et al., 2007).

At the east margin of Amery Ice Shelf area, the zircon U–Pb ages reveal both evidence of 2582 Ma Neoarchean crust (Black et al., 1991) and 531 to 545 Ma high-grade metamorphic events (Liu et al., 2007a). Sillimanite bearing pegmatite provides a monazite U–Th–Pb age of 536 ± 17 Ma (Ziemann et al., 2005). The rutile and titanite U–Pb age from light color gneiss at Austin Nunatak is 510 to 508 Ma (Mikhalsky et al., 2001).

In the McKaskle Hills area of the north Amery Ice Shelf, residual zircon cores give ages of 1174 to 932 Ma for orthogneiss, granulite, and paragneiss (Liu et al., 2007b). Euhedral zircon grains and zircon rims give ages of 545 to 529 Ma (Liu et al., 2007b).

2.2. Grove Mountains geology

The Grove Mountains are comprised of a group of about 64 nunataks exposed in a 3200 km^2 ice covered area between the Southern and Northern Prince Charles Mountains and Larsemann Hills (72°20′–73°10′S and 73°50′–75°40′E) (Fig. 1). These nunataks are structural highlands that formed during late Mesozoic to Cenozoic high angle normal faulting (Hu et al., 2008). The nunataks, usually 100–200 m in height, align generally in NNE–SSW direction, form five island chains, and produce ridge and valley topography. The northwest sides of the nunataks are usually exposed as vertical cliffs reflecting nearly vertical high-angle fault surfaces.

In the nunataks to the east of Grove Mountains, such as Mount Harding, Zakharoff Ridge, Davey Nunatak, Wilson Ridge, and Gale Escarpment, about 55% of exposure consists of light color granulite and charnockite. About 15% of granulite outcrops contain dark bands of plagioclase–amphibolitic gneiss. In the nunataks to the west of Grove Mountains, such as Melvold, Mason Peaks, Truman and Black Peaks, approximately 60% of the outcrop consists of light colored, medium to coarse grain granitic gneiss. Some light color granulite bands are found in the gneiss at the Black Peaks outcrops. Dark colored, thin layers or lenses of mafic granulites, which are generally several centimeters to 20 m in thickness, are distributed as inclusions in the light color granulite and granitic gneiss.

Pink porphyritic K-feldspar granitic veins intruded the gneiss along foliation. The granitic veins are widespread and form about 20% of outcrops. The majority of granitic veins are distributed over the Davey Nunataks and the middle segment of Gale Escarpment.

Orthopyroxene–garnet–biotite–cordierite plagiogneiss and a narrow layer of spinel–garnet–biotite plagiogneiss were found at Bryse Peaks and to the north of Wilson Ridge. They are the major metasedimentary rocks in the Grove Mountains.

Granodiorite, granitic aplite, and pegmatite dykes are widespread and intrude all major lithologies. The dikes are usually 0.5 to 20 m wide. The planar structures in the country rock are truncated at high angle by the dikes (Liu et al., 2003).

The rocks in the Grove Mountains mainly record two major thermal events; one at 920–910 Ma (Hensen and Zhou, 1995; Zhao et al., 1995; Kinny, 1998; Wang et al., 2003; Kelsey et al., 2007) and the other at 570 to 507 Ma (Zhao et al., 2000; Mikhalsky et al., 2001; Liu et al., 2006, 2007b, 2009a; Harley et al., 2013). The mineral and whole-rock Sm–Nd isochron ages for granulites are 536 ± 3 Ma (MSWD = 0.67) and 507 ± 30 Ma (MSWD = 4.6). Initial $^{143}Nd/^{144}Nd$ ratios (I_{Nd}) are 0.511450 ± 0.000015 and 0.51130 ± 0.00005, respectively (Liu et al., 2006, 2007b). The 570–545 Ma HP granulite metamorphism may be related to a subduction–collision tectonic event along the Prydz Belt (Liu et al., 2009a).

3. Morainal deposits in the Grove Mountains

The movement of glaciers around the nunataks generated several elongate gravel rich moraines (Fig. 2a, b). There are five moraines to the west of Gale Escarpment (EP): one along each side of the N–S trending Mount Harding (HD) and another to the south of Mason Peaks. The west Mount Harding moraine originates at the southern margin of Mount Harding. The eastern slope of Mount Harding extends about 5 km and connects to the north nunataks of the Gale Escarpment and to the south nunataks of Zakharoff Ridge (Fig. 1).

Morainal boulders may be larger than several meters in size, but the majorities are less than 50 cm. There is observable sorting from the center to the edge of the morainal belts; similar size pebbles line up roughly parallel to the long direction of both the morainal belt (Fig. 2a, c).

The gravels are less sorted and contain larger boulders adjacent to the nunataks. Pebbles larger than 50 cm are mainly found within 100 m of the nunataks (Fig. 2d). Farther from the nunataks, particle size decreases to about a mean of 0.5 cm and small pebbles and sand

predominate. Most of the large blocks are similar in composition to the exposed bedrock and are mainly charnockite, felsic orthogneiss, mafic granulite, porphyritic K-spar granite, and garnet felsic gneiss. High-pressure mafic granulite and ultramafic rock are found in the gravel but have not been identified in bedrock. The detrital samples for this study were collected from gravels containing small pebbles to sand (Fig. 3a, b).

Tillite pebbles (Fig. 3c) in the moraine range from several centimeters to 30 cm and are in various stages of disintegration. The rock clasts in tillite are gneiss, charnockite, and mafic granulite. Mineral and rock fragments are distributed in grayish green silt cement with laminar structure. Tillite pebbles show evidence of wind erosion and have subrounded shapes. They formed in the sediments at the terminus of the glacier (Fang et al., 2004a). Based on pollen studies, the tillite age is about 3.5 Ma and formed during Pliocene glacial retreat (Liu et al., 2001; Li et al., 2003a; Fang et al., 2004a,b).

Paleosol occurs in Mount Harding area with the largest exposure about 1 km^2 in area (Li et al., 2003b). The paleosol belongs to the alpine frost desert soil type, with high salt, weaky acidic, and organic free character and belongs to weathering stage 3 to 4 (Campbell and Claridge, 1987). The paleosol formed at 3.5 to 0.5 Ma based on the soil structure (Li et al., 2003b). The Mount Harding paleosol formed in dry conditions and did not experience strong chemical weathering. The mineralogical character and detrital zircon ages determined from the paleosol should provide information about bedrock composition and age.

4. Results

4.1. Sampling and testing method

Four samples were collected for zircon chronology. 1) Samples of fine-grained gravel to sand were collected from the west side of Gale Escarpment (EP21-1) and from the west flank of Mount Harding (HD17-1). Five kilograms of particles was gathered near large morainal boulders for each sample. A quarter of the splits were used to select zircon. 2) A solidified tillite sample was collected from the west side of Mount Harding (LMK23). The tillite sample was crushed and then divided to separate the zircon. 3) A paleosol sample was collected at Mount Harding (NJ02) (Fig. 3). Zircons were separated from the entire soil sample.

Zircon grains were separated by conventional magnetic and heavy liquid procedures, and handpicked under a binocular microscope. They were mounted in epoxy and polished until the grain centers were exposed. Prior to analysis, reflected light photomicrographs and cathodeluminescence (CL) images were obtained to investigate the zircon characters.

The zircon U–Pb dating was completed with a LA-ICP-MS in the Continental Dynamics Laboratory, Northwest University, Xi'an, China. The laser ablation system is a Geolas200M manufactured by the Mocrolas Company, Germany. Analyses used a 30 μm beam, 20–40 μm ablation depth, 10 Hz laser pulse and 34–40 mJ energy. The ICP-MS system is an Agilent 7500Va. Standard ISO91500 was used as the external standard to bracket the age data, with one standard analysis after the analysis of every five samples for instrument bias correction. For every 20-zircon analyses, standard NIST610 was analyzed twice to measure the U, Th, and Pb contents based on the SiO_2 content as an internal standard. For zircon trace element analyses, isotope data processing, and age calculation, the GLITTER method was used. The common Pb correction is based on the Andersen (2002) method, and ages were calculated by the ISOPLOT2.06 program (Ludwig, 1999). Detailed analysis procedure and data processing follow the methods of previous workers (Gao et al., 2002; Yuan et al., 2004).

The mineralogical characters of the detrital samples were compared with that of the local exposed bedrock. Mineral chemistry was obtained from University of Texas at El Paso on a Cameca SX50 and University of Nevada Las Vegas on a JEOL JXA-8900. Analysis conditions were 15 kV accelerating voltage, 20 nA beam current, 5 μm beam size, and 30 s peak counting time. Calibration standards include Astimex chromite for Cr; fluorite for F, tugtupite for Cl, marcasite for S, apatite for P. Smithsonian diopside for Si, Mg, and Ca; anorthoclase for Al and Na; microcline for K; ilmenite for Ti and Fe. A set of standards from both the Smithsonian and Structure Probe, Inc. (SPI) was analyzed repeatedly to monitor the accuracy and precision of the analyses.

4.2. Petrography

Bedrock samples were collected from the Gale Escarpment (EP), Mount Harding (HD), and Zakharoff Ridge (ZK). The rocks from Gale Escarpment are mainly slate, schist, amphibolite, granulite, and gneiss. The rocks from Mount Harding are slate, granitic schist, granitic gneiss, charnockite, and granite. Two rock samples from Zakharoff Ridge (ZK) are slate and granite. Igneous rocks from Davis (dvs) are diorite, amphibolite, and trachyte. The petrography for both detritus and bedrock samples is summarized in Tables 2 and 3.

Four thin sections of gravel to sand fragments from the Gale Escarpment (EP21-1-2, 7, 8, 12) were analyzed. Grain size in these samples varies from 0.2 to 3 to 4 mm. The 0.2 to 1 mm size range mainly contains mineral chips. With an increase of grain size, there are more rock fragments. The identifiable rock fragments are diorite, granite, amphibolite, gneiss, and fine grain meta-sandstone. Mineral distribution in EP glacial debris is as following: K-feldspar 25%, plagioclase 16%, amphibole 15%, quartz 15%, biotite 10%, magnetite/hematite 5%, orthopyroxene 3%, garnet 3%, ilmenite 2%, cummingtonite 1%, clinopyroxene less than 1%, and minor zircon, titanite, and epidote.

Five thin sections were analyzed for the fine grain gravel and sand fragments from the west flank of Mount Harding (HD17-1-1, 2, 5, 6, 7). Grain size ranges from 0.5 to 5 mm. For the less than 1 mm size range, grains are mainly quartz, feldspar, biotite, and amphibole, with a few granite and fine grain meta-sandstone fragments. The amphibole grains clearly show two types, one with light yellow to light green

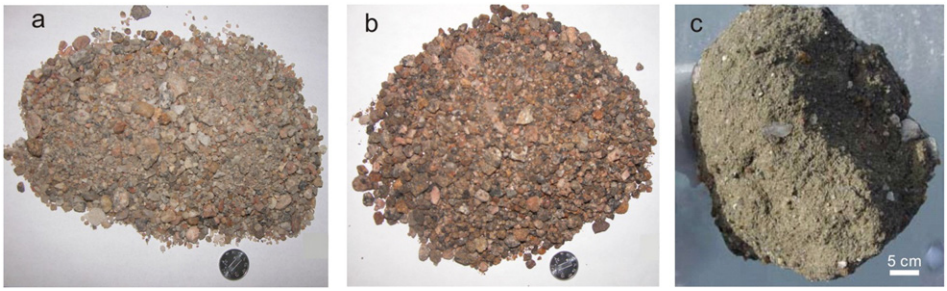

Fig. 3. Samples used for the detrital zircon U–Pb dating and the detrital mineral microprobe analysis. a: the sand and fine-gravel sample (EP21-1) from #1 morainal belt to the west of south Gale Escarpment; b: the sand and fine-gravel sample (HD17-1) from the morainal belt to the west of Mountain Harding; c: the semi-consolidated tillite sample (LMK23) from the morainal belt to the west of Mountain Harding. The diameter of the coin is about 2 cm.

Table 2
Characters of morainal detritus of Grove Mountains, East Antarctica.

Location	Sample #	Grain size range (mm)	Grain type	Characters
Gale Escarpment	Ep21-1-2	0.2 to 1	Minerals	qz 25% + pl 30% + kf 25% + amph 10% + bio 10% Half qz + fs grains, half rock fragments
	Ep21-1-7	1 to 2	Minerals + rocks	Rocks: diorite, amphibolite, and granite The amphiboles show different pleochroism for diorite and amphibolite. Half mineral grains (qz + fs + amph), half rock fragments.
	Ep21-1-8	1 to 2	Minerals + rocks	Rocks: gneiss, diorite, and granite. Gneiss: amph + bio + pl, biotite aligned. Diorite: amph + pl + mafics, medium size grain. Granite: fs + qz + bio, fs has clay alteration. Half qz + fs grains, half rock fragments.
	Ep21-1-12	2 to 4	Minerals + rocks	Rocks: amphibolite, granite, and meta-sandstone. Amphibolite: amph + pl with qz corrosion Granite: fs + qz + amph Meta-sandstone: fine grain (<0.2 mm) fs and qz tightly wedged together
Mount Harding	Hd17-1-1	2 to 5	Minerals + rocks	The minerals are mainly qz + pl + amph + cpx. The rock fragments are mainly the similar type — slate. The fine grain qz + pl + bio + oxides + amph are tightly wedged together with linear orientation. About 60% mineral grains with 40% rock fragments.
	Hd17-1-2	1 to 3	Minerals + rocks	The minerals are mainly qz + pl + kf. Rocks: slate and granite Slate: fine grain with qz + pl + kf + bio Granite: medium grain with qz + pl + kf + bio Minerals have qz + fs + amph + bio
	Hd17-1-5	Around 1	Mainly mineral grains	Amphiboles have two types, one with green to brown pleochroism, and another with bluish green to pale green pleochroism. Minerals have fs + qz + amph + bio
	Hd17-1-6	0.5 to 1	Mainly mineral grains	Amphiboles mainly have green to light brown pleochroism Rocks: granite, diorite, and slate Diorite: medium grain with amph + pl Granite: medium grain with fs + qz + bio + amph Slate: fine grain (0.2 to 0.3 mm) with qz + fs + bio and a few rock fragments
	Hd17-1-12	1 to 2	Minerals + rocks	Half mineral grains and half rock fragments. Minerals have qz + fs + bio + cpx Rocks: sandstone, amphibolite, slate, and granite. Sandstone: medium grain with mainly qz + fs Amphibolite: medium grain with amph + pl + oxides. Slate: fine to medium grain with fs + qz + bio with linear structure. Granite: medium grain with fs + qz + bio + amph. Minerals include: fs + qz + bio + amph The amount of bio and amph are less than 20%.
Tillite from the west bank of Mount Harding	LMK23-2	0.5 to 1	Mainly minerals	Rock: granite and meta-sandstone Granite: fine to medium grain, fs + qz + bio, Meta-sandstone: fine grain, mainly fs + qz. Similar as the LMK23-2.
	LMK23-3	0.5 to 1	Mainly minerals	Rocks: granite, granulite Granite: fine to medium grains wedged together, mainly fs + qz + bio Granulite: fine grain, grain size 0.1–0.3 mm, pl + qz + cpx + bio Minerals are mainly qz and fs
	LMK23-6	1 to 3	60% minerals 40% rocks	Rocks; granite, meta-sandstone. slate, granulite Granite: medium grain, fs + qz + bio + oxide Meta-sandstone: medium grain, qz + fs Slate: fine grain, fs + qz + bio with linear structure Granulite: this is the major type of rock fragments, fine anhedral grains (<0.5 mm) wedged together, fs + qz + cpx + bio
	LMK23-9	0.1 to 0.5	Minerals	Fs 40%, qz 15%, amph 25%, oxide 10%, bio 5%, cpx 5%. Amphiboles mainly have dark green to brownish green pleochroism
Paleosol from Mount Harding	NJ02	0.2 to 5 mm grains in nanometer size matrix	Mainly minerals	The large grains (>1 mm) are almost all qz + fs Fs 40% + qz 30% + amph 20% + bio 5% + oxide 5%, some fs are microcline with cross twining. The size of mafics and oxides are usually < 0.5 mm. Amphiboles are mainly have bright bluish green to dark green pleochroism. For three thin sections, the following rock fragments may exist: Granite: medium grain with fs + qz wedged together. Granite: medium grain with microcline + plagioclase + biotite, with wormy quartz. Amphibolites: medium grain pl + amph + qz, amphiboles mainly have green to yellowish green pleochroism. Meta-sandstone: fine grain, fs + qz wedged together.

amph: amphibole; bio: biotite; fs: feldspar; kf: K-feldspar; pl: plagioclase; qz: quartz; cpx: clinopyroxene.

pleochroism and another with light yellowish green to dark green pleochroism. With the increase of grain size, more rock fragments are preserved. The identifiable rock fragments are fine grain meta-sandstone, granite, diorite, and amphibolite. The mineral distribution is as follows: K-feldspar 20%, amphibole 18%, quartz 15%, plagioclase 10%, biotite 9%, orthopyroxene 9%, ilmenite 7%, magnetite/hematite 6%, apatite 3%, cummingtonite 1.5%, zircon 1%, clinopyroxene less than 1%, and one grain of garnet.

Four thin sections were analyzed for fine-grained gravel to sand fragments from solidified tillite from the west side of Mount Harding

Table 3
Petrographic characters for Grove Mountains bedrocks, East Antarctica.

Location	Sample #	Rock type	Petrographic characters
Gale Escarpment	Ep 1-1	Amphibolite w/ gabbro vein	Minerals: amph 70% + pl 20% + bio 10% + grt 5% Minerals are medium size with anhedral shape and linear structure, anhedral garnet grains are surrounded by fine grain plagioclase. A few orthopyroxenes included amphiboles. The gabbro vein composed by large pl (70%) and opx (30%), a few cpx.
	Ep 1-9	Amphibolite	Minerals: amph 60% + cpx 20% + pl 15% + grt 5% Coarse grain, amph is around 1 to 2 mm in size and pl is around 0.5 mm. Anhedral grt within pl clusters.
	Ep 2-1	Gneiss	Minerals: pl 60% + bio 15% + opx 10% + amph 10% + grt 5% + opaque Medium size grains around 0.3 to 1 mm. Mafic minerals for linear structure, pl forms the augen lens within mafic bends.
	Ep 2-2	Schist	Minerals: fs 50% + qz 20% + bio 10% + opx 10% + amph Fine grain (~0.5 mm) with linear structure, bio and opx form +bending, fs and qz form equigranular texture.
	Ep 16-5	Amphibolites w/pegmatite vein	Amphibolite is medium grain (~1 mm) with linear structure. Minerals: fs 30% + qz 30% + amph 30% + bio 10%. Pegmatite: large microcline with pl and qz inclusions, wormy texture for pl next to K-spar.
	Ep 24-4	Amphibolite	Medium grain (~1 mm) with linear structure, equigranular pl and qz for elongated lens within the mafic mineral bends. Minerals: opx 20% + amph 20% + pl 40% + qz 20% + cpx <5% + bio <5% + opaque
	Gep 2-4	Amphibole granitic gneiss w/ gabbroic vein	There are two layers in this sample, one with mineral assemblage of bio 35% + amph 20% + pl 35% + opaque, the other with mineral assemblage opx + bio + pl. Medium grain (1 to 2 mm) with linear structure Minerals: amph 20% + bio 40% + pl 35% + opaque 5%
	Gep 2-6	Amphibolite	Coarse grain (~2 mm) with linear structure, mafics form the dark bend and plagioclase for elongated lens
Mount Harding	Hd 2-1	Slate	Minerals: fs 60% + qz 30% + bio 10% Fine grain with biotite forming linear structure. Felsic minerals are equigranular with round quartz punching in feldspars. Minerals: kf 35% + Pl 35% + qz 15% + bio 5% + opx 5%, all in anhedral shape
	Hd 8-2	Charnockite	Coarse grain (2–3 mm) with equigranular texture. Minerals: kf 40% + pl 30% + qz 10% + bio 10% + opaque
	Hd 9-1	Slate	Fine grain (~0.5 mm), feldspar and quartz form equigranular texture, biotite and opaque orientate to form the linear structure. Minerals: fs 45% + qz 20% + amph 15% + opx 10% + bio 5% + opaque 5%
	Hd 9-4	Granitic gneiss	Medium grain (1–2 mm), felsic grains form the augen lens within mafic bends. Minerals: kf 55% + pl 15% + qz 20% + bio 5% + opaque
	Hd 9-5	Granite	Coarse anhedral grain (3–5 mm) with equigranular texture. Biotites are smaller (<1 mm) between felsic grains, half biotite oxidized. Minerals: kf 50% + pl 10% + qz 35% + garnet
	Hd 24-1	Granite	Coarse anhedral grains wedged together. Most of kf show perthitic texture, the exsolutions show as thin lines. Some feldspars have wormy texture.
Zakharoff Ridge	Zk 7-1	Granite	Coarse anhedral grains are wedged together, some K-feldspars have perthitic texture, some pl have wormy structure. Minerals: kf 45% + ab 15% + qz 30% + bio 5% + opaque + garnet
	Zk 9-2	Slate	Fine grain (~0.5 mm) with linear structure. Biotite and opaque line up. Minerals: fs 50% + qz 40% + bio 10% + a few opaque
Davis	Dvs 1-1	Trachyte	Plagioclase (0.5–2 mm) forms a pilotaxitic texture, amphibole and opaque filled between the plagioclase grains Minerals: pl 50% + amph 40% + opaque 10%
	Dvs 1-2	Porphyritic trachyte	Phenocryst: 0.5–2 mm subhedral pl, 10% parallel aligned Matrix: holocrystalline texture, 0.2 mm size pl 40% + amph 40% + opaque 10% form linear structure Minerals: amph 40% + pl 30% + qz 10% + opx 10% + bio 5% + opaque
	Dvs 1-3	Amphibolite	The rock has a mylonitic structure, majority amph, pl, and qz have changed to 0.1 mm size grains. The rock still keeps the original bending structure, mafic and felsic minerals form bends. Opx are generally in the center of amph and did not mylonitize. Minerals: pl 50% + amph 40% + opaque 10%
	Dvs 1-4	Trachyte	Plagioclase (0.5–2 mm) forms a pilotaxitic texture, amphibole and opaque filled between the plagioclase grains Minerals: pl 50% + amph 40% + opaque 10%
	Dvs 1-5	Trachyte	Plagioclase (0.5–2 mm) forms a pilotaxitic texture, amphibole and opaque filled between the plagioclase grains Minerals: microcline 40% + pl 20% + qz 20% + mus 15% + bio 5%
	Dvs 1-7	Granite	Coarse grain (>5 mm), some K-feldspars have thin perthitic stripes.

amph: amphibole; bio: biotite; fs: feldspar; kf: K-feldspar; ab: albite; pl: plagioclase; qz: quartz; cpx: clinopyroxene; opx: orthopyroxene; mus: muscovite; grt: garnet.

(LMK23-2, 3, 6, 9). The mineral assemblages are: K-feldspar 18%, orthopyroxene 18%, quartz 16%, plagioclase 15%, biotite 8%, amphibole 8%, ilmenite 9%, magnetite/hematite 7%, clinopyroxene 1%, less than 1% garnet, and less than 1% apatite, zircon, and monazite.

Three thin sections were studied for the fine grain paleosol from Mount Harding (NJ02-a, b, c). The paleosol has a greenish color with fine grain mineral fragments distributed in a nano-size matrix. The mineral fragments are 0.1 to 0.3 mm in size and have angular shapes. They include: K-feldspar 27%, plagioclase 25%, amphibole 16%, quartz 14%, garnet 6%, magnetite/hematite 4%, ilmenite 2%, clinopyroxene 2%, biotite 1%, orthopyroxene 1%, and less than 1% of zircon, titanite, and apatite.

4.3. LA-ICP-MS detrital zircon U–Pb age

Gale Escarpment (EP21-1) zircons are euhedral to subhedral (Fig. 4). The elongated grains lack clear growth zoning and might be the product of metamorphism. The short prismatic grains typically show weak zoning and may represent magmatic zircons. Mount Harding (HD17-1) zircons are subhedral, with short prismatic to rounded shapes. Most of the grains are zoned, and some grains have a thin bright rim. Some grains have a clear rounded core. The zircons from solidified tillite (LMK23) are similar to the Gale Escarpment zircons with elongated shape. The zircons from the paleosol sample (NJ02) are generally small (<100 μm) and typically have rounded edges and zoning.

The separated zircon grains from four detrital samples were analyzed for U–Th–Pb contents by LA-ICP-MS and the results are provided in Supplementary material I (S I). Analyses are mainly taken from the center of zircon grains, except for strongly zoned zircon (Fig. 4). Clear 550–500 Ma age peaks are observed in the histograms of all 4 samples. Most of zircon ages at 550–500 Ma have high concordance; therefore, these $^{206}Pb/^{238}U$ ages should be reliable and the age histograms are plotted using $^{206}Pb/^{238}U$ ages. The ages for each sample are described below.

A total of one hundred twenty zircon ages were determined for the sample from the west of the Gale Escarpment (EP21-1). Twelve spots with concordance less than 50% were not reported. The other one hundred and eight ages range from 460 ± 3 Ma to 2335 ± 15 Ma. Among them, 23 spots have concordance less than 85% (with 4 of them less than 70%). In the concordia diagram (Fig. 5), most of the discordant zircons fall on an array projecting to 1100 Ma. Some outliers are in the 700–800 Ma range. In the age histogram plot (Fig. 5), one peak of 64 points falls between 450 and 550 Ma (weighted average at 530 Ma), which account for 53% of all points. Another peak of 21 points is between 800 and 910 Ma, which counts for 17.5% of all points. There is a small peak at 700 Ma containing 6 data points. Two zircon ages fall between 2300 and 2420 Ma.

A total of one hundred twenty seven zircon ages were determined from the sample collected to the west of the Mount Harding gravel belt (HD17-1). Seventeen spots with concordance less than 50% are not included in the reported data. The other one hundred ten spots yielded ages ranging from 225 ± 2 Ma to 992 ± 7 Ma. Among them, 42 spots have concordance less than 85% (with 3 of them less than 70%). In the concordia diagram (Fig. 5), most of the discordant zircons fall on an array projecting to 1000 Ma. Some outliers are in the 800–900 Ma age range. In the age histogram plot (Fig. 5), there are 114 points distributed between 450 and 870 Ma, accounting for 89.76% of the data. These points produce three peaks, the first contains 50 data points (44%), distributed between 450 and 560 Ma (weighted average at 510 Ma). The other two peaks have 7 and 13 data points at 700 Ma and between 830 and 870 Ma respectively. Other data points fall mainly below 400 Ma with several about 1000 Ma.

A total of ninety points were analyzed for the zircons from the west Mount Harding tillite sample (LMK 23). Five spots with concordance less than 50% are not reported. The other eighty-five spots yielded ages ranging from 434 ± 3 Ma to 1158 ± 8 Ma. Among them, 26 spots have concordance less than 85% (with 3 of them less than 70%). In the concordia diagram (Fig. 5), most of the discordant zircons fall on an array projecting to 1000 Ma. In the age histogram plot (Fig. 5), 77 points fall between 440 and 600 Ma (peak at 500 Ma), accounting for 85.6% of the total. Other points distribute between 800 and 1000 Ma. One point falls at 1200 Ma.

A total of one hundred twenty zircon dates were obtained from Mount Harding paleosol sample (NJ 02). Ten spots with concordance less than 50% are not reported. The other one hundred ten spots yielded

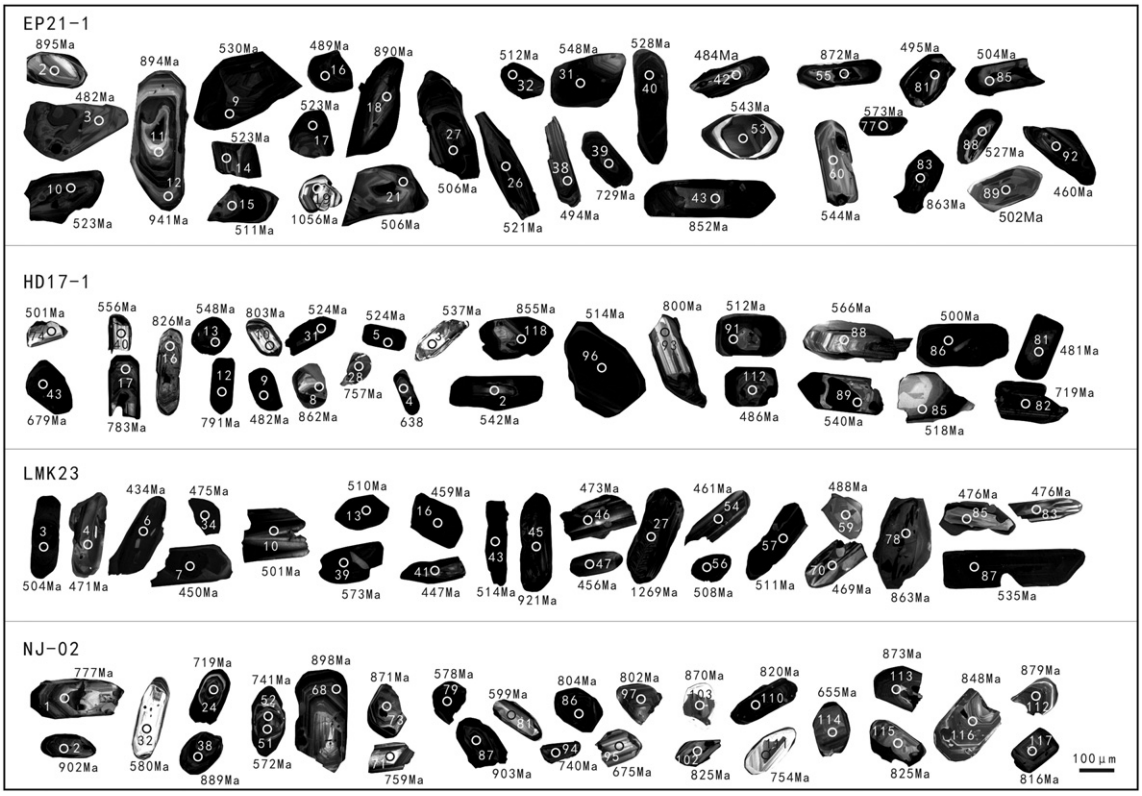

Fig. 4. Zircon CL images and LA-ICP-MS spot locations. The circles and numbers in the Zircons are the locations and analysis numbers of the laser ablation spot, and the numbers out of the Zircons are the calculated age from LA-ICP-MS analyses. EP21-1: zircons from #1 morainal belt to the west of south Gale Escarpment; HD17-1: zircons from morainal belt to the west of Mount Harding; LMK23: zircons from consolidated-semi consolidated tillite to the west of Mount Harding; NJ-02: zircons from paleosol sample in Mount Harding.

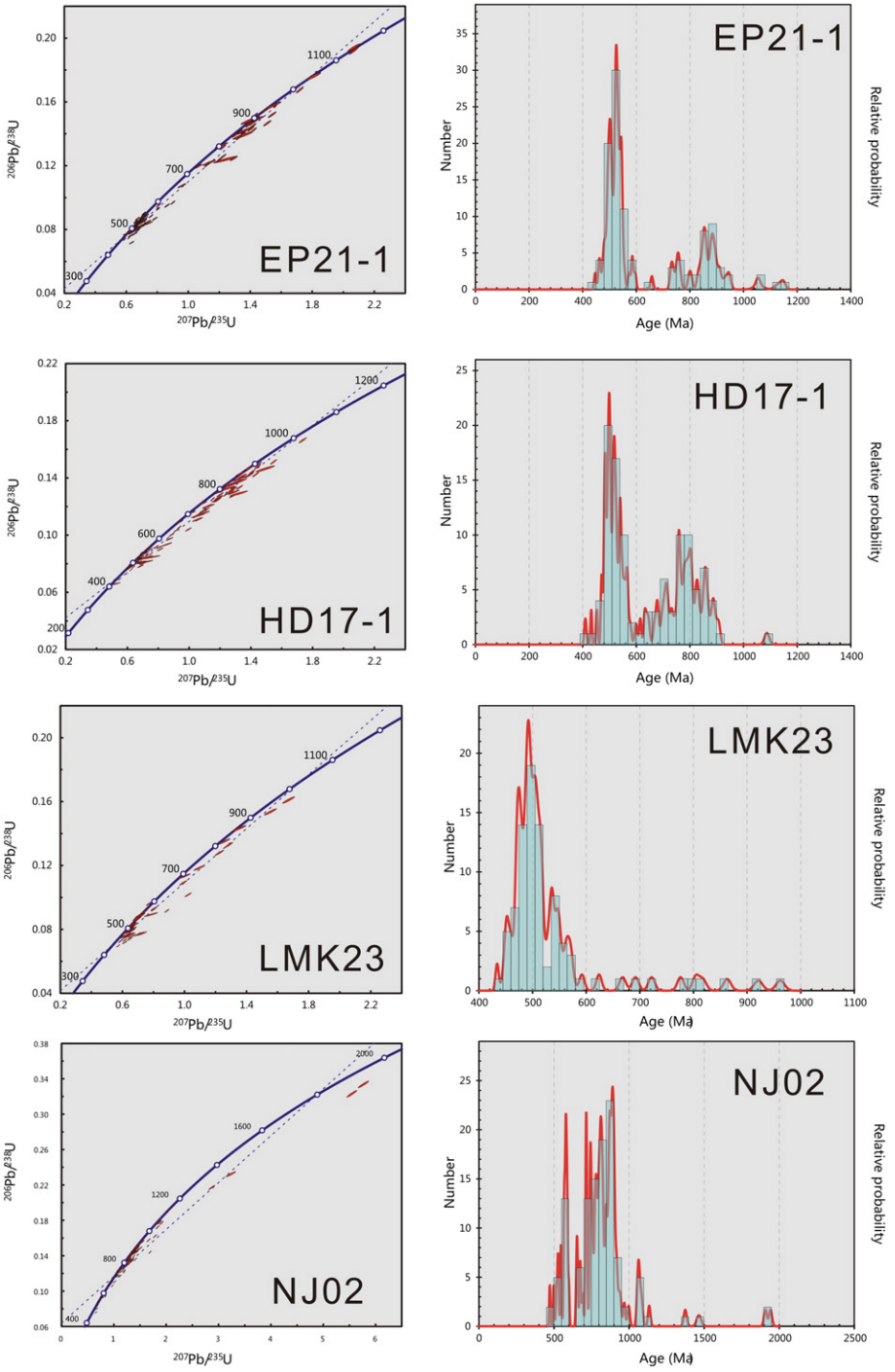

Fig. 5. Detrital zircon LA-ICP-MS ages for EP21-1, HD17-1, LMK23, and NJ-02. Left column shows the concordia diagrams of all LA-ICPMS $^{207}Pb/^{235}U$ vs. $^{206}Pb/^{238}U$. Right column shows the histograms of ages for the four samples.

ages ranging from 472 ± 2 Ma to 1856 ± 7 Ma. Among them, 20 spots have concordance less than 85% (with 1 of them less than 70%). In the concordia diagram (Fig. 5), most of the discordant zircons fall on an array projecting to 1200 Ma, but another possible discordant array projects to 2000 Ma. Some outliers occur in the 800–900 Ma range. In the age histogram plot (Fig. 5), there are two peaks at 460–640 Ma (peak at 560 Ma) with 26 points (21.7%) and 700–940 Ma (peak at 860 Ma) with 70 points (58.3%). Fourteen points (11.7%) form a weak peak between 940 and 1160 Ma. Other points fall at 1300 Ma, 1470–1600 Ma, 1800 Ma, 2000 Ma, and 2600 Ma.

4.4. Mineral chemistry

The mineral compositions for morainal samples and bedrock were analyzed by EPMA. Results for the morainal samples are in Supplementary material II (S II). Bedrock mineral chemistry is in Supplementary material III (S III). The Gale Escarpment high-pressure mafic granulite (ep-HP-MG) mineral compositions are from Liu et al. (2009a) and include minerals from unaltered, weakly retrograded, and strongly retrograded granulites. The minerals from high grade metamorphic rocks (mainly ecologite) in East Antarctica (EA-HP-rk) (Peacock and

Goodge, 1995; Di Vincenzo et al., 1997; Board et al., 2005; Palmeri et al., 2007; Romer et al., 2009; Godard and Palmeri, 2013) and minerals of basement rocks from Prydz Bay area (Prydz-BR) (White and Clarke, 1993; Carson et al., 1996; Harley et al., 1998; Boger et al., 2002; Boger and White, 2003; Kelsey et al., 2003a; Kelly and Harley, 2004; Boger and White, 2005; Tong and Wilson, 2006; Liu et al., 2007a,b; Phillips et al., 2007, 2009) have been compiled for comparison. The mineral compositions from both diamicton (15 mounted thin sections from splits of 4 samples) and bedrock (27 samples) were compared with published data to identify the possible source regions of the morainal deposits.

The comparisons of major mineral compositions between detrital samples, bedrock and compiled data (Fig. 6) are as follows:

4.4.1. Garnet (grt)

Garnets are mainly found in Gale Escarpment (EP) detritus (ep-sd) and Mount Harding (HD) paleosol samples (nj-sd); only few garnets exist in Mount Harding (HD) detritus (hd-sd) and solidified tillite (lmk-sd). In the studied Gale Escarpment bedrock samples, only amphibolite (ep-rk) contains garnet. Gneiss and schist do not contain garnet. The garnet from EP amphibolite forms a narrow compositional cluster (Fig. 6a). Garnet is a major mineral in the Gale Escarpment (EP) high-pressure mafic granulite (Liu et al., 2009a). In Mount Harding and other areas, garnets mainly exist in granitic bedrock (hd-rk, dvs-rk, and zk-rk).

The FeO/(FeO + MgO) ratio, (FeO*), CaO, and MnO contents of the garnets show clear compositional variations (Fig. 6a). Detrital garnets are generally different in composition from the bedrock garnets. Garnets from EP and HD bedrock (ep-rk and hd-rk) have higher MnO contents and plot outside of the Prydz-BR field.

All the garnets from granitic bedrock from Mount Harding (hd-rk), Zakharoff Ridge (zk-rk), and Davis (dvs-rk) form their own clusters. The composition of detrital garnet is distinct from garnet from granitic bedrock. Only the garnets from the paleosol overlap with those from granite bedrock. However, the garnets from granites still fall near the field of garnet composition compiled from Prydz Belt bedrock (Prydz-BR), except the Mount Harding granite. The garnets from Gale Escarpment amphibolite bedrock (ep-rk) are outside the Prydz Belt bedrock field.

Orthopyroxene (opx): Opx is common in EP (ep-sd) and HD (hd-sd) detritus and solidified tillite (lmk-sd) but is rare in paleosol (nj-sd). The bedrock opx forms clusters based on their locations (Fig. 6a). Most HD detrital opx is similar to HD bedrock opx but has a broader compositional range. EP detrital opx and paleosol opx are less common, generally more Mg rich, and distinct from all bedrock opx. EP bedrock opx is generally different from HD opx (both detrital and bedrock). There is a few opx reported in Gale Escarpment high-pressure mafic granulite (ep-HP-MG) (Liu et al., 2009a), and it show similar chemistry to EP detritus. Most opx from the Grove Mountains area has lower Al_2O_3, higher MnO and FeO* compared to EA-HP-rk and Prydz-BR. They plot mostly outside or on the edge of the Prydz-BR field.

4.4.2. Clinopyroxene (cpx)

Cpx is occasionally found in detritus and generally has high MnO contents (Fig. 6a). Detritus cpx is generally different from cpx in bedrock. In the studied bedrock samples, only some EP amphibolites (ep-rk) contain cpx and have different chemistry from the Prydz-BR cpx (gray field in Fig. 6a). Cpx is common in EA-HP-rk, however, it is rarely reported in Prydz-BR. The cpx compositions from EA-HP-rk form three clusters, which may correspond to different sources. Cpx from Davis trachyte falls in Prydz-BR cpx field (Fig. 6a).

4.4.3. Amphibole (amph)

Amphibole is the most common mineral in detritus other than feldspar. Generally, amphibole in EP detritus and paleosol is similar and has higher MgO but both EP detritus and paleosol are different in composition compared to amphibole in HD detritus (Fig. 6b). Compared with EA-HP-rk and Prydz-BR, amphibole from detritus is more MnO rich. Amphibole from bedrock forms clusters and some plot in the Prydz-BR field. Amphibole in EP-HP-MG from Grove Mountains (Liu et al., 2009a) plots partially within the EA-HP-rk field.

4.4.4. Cummingtonite

There are a few Fe–Mg amphiboles found in EP and HD detritus. Their compositions can be divided into two groups, FeO* about 0.45 wt.% and FeO* in the 0.7–0.8 range. There is no cummingtonite data reported for the Prydz Bay area.

4.4.5. Biotite (bio)

Biotite in EP detritus is clearly different from biotite in HD detritus (Fig. 6b). Biotite from EP detritus has higher Al and Mn contents and most of them are clearly different from biotite in the local bedrock. Biotite in HD detritus and tillite are similar to biotite in bedrock. The biotite in the Prydz-BR generally has lower MnO and higher Al_2O_3 than the biotite from this study. Zakharoff Ridge (zk-sd) biotite is similar in composition to those in HD rocks. Only one granitic rock from Davis contains biotite. This biotite is distinctive and falls in Prydz-BR biotite field.

4.4.6. Fe–Ti oxides and Fe oxides

Oxide contents in EP detritus are lower than that in HD detritus. Some ilmenite from HD shows slight alteration and has higher Ti content (Fig. 6b). This high Ti ilmenite is also occurs in HD detritus and tillites. Generally, ilmenite from this study has lower Mn and higher Mg than ilmenite from Prydz-BR.

4.4.7. Plagioclase

Because of the broad compositional range between Na and Ca end-members in the studied plagioclases, it is difficult to compare the plagioclase.

4.4.8. K-feldspar

K-feldspar is either microcline or perthite (Fig. 7). There are two types of perthite in EP detrital grains; albite forms droplets within orthoclase and albite forms thin laminae in orthoclase (EP21-1). For bedrock in the EP area, the laminal shape of albite exsolution is more common (EP2-2, EP16-5, and GEP2-4). Perthitic feldspar is less common in the HD detritus. In these samples, albite mainly forms thin laminal stripes and rounded droplets (Hd17-1-6, 7). In the HD bedrock, perthite mainly occurs in HD24-1 granite and the albite exsolutions form narrow-elongated lens and droplets in K-feldspar. In Zakharoff Ridge granites (ZK7-1), perthite is common. In all other HD bedrock samples, K-feldspar shows weak exsolution features (LMK23, Hd8-2, Hd9-1).

5. Discussion

5.1. Source region of morainal detritus

The major detrital minerals, such as garnet, orthopyroxene, clinopyroxene, amphibole, and biotite, show broad chemical variations (Fig. 6a, b). The majority of morainal and paleosol garnets fall in the garnet field compiled from Prydz Bay basement rocks (Prydz-BR) (Fig. 6a). Some high MnO garnets in detritus are similar to garnets in the metapelite from the Ruker Province (Phillips et al., 2007) or the garnets in altered pegmatites from the northern Prince Charles Mountains (Boger et al., 2002). Several EP detrital garnets plot adjacent to the HP mafic granulite group. Garnets from Gale Escarpment high pressure mafic granulite (ep-HP-MG) (Liu et al., 2009a) and some garnets from EP detritus and HD paleosol fall in the garnet field of East Antarctica high pressure rocks (EA-HP-rk) in both FeO*–CaO and FeO*–MnO plots but they have higher CaO contents (Fig. 6a).

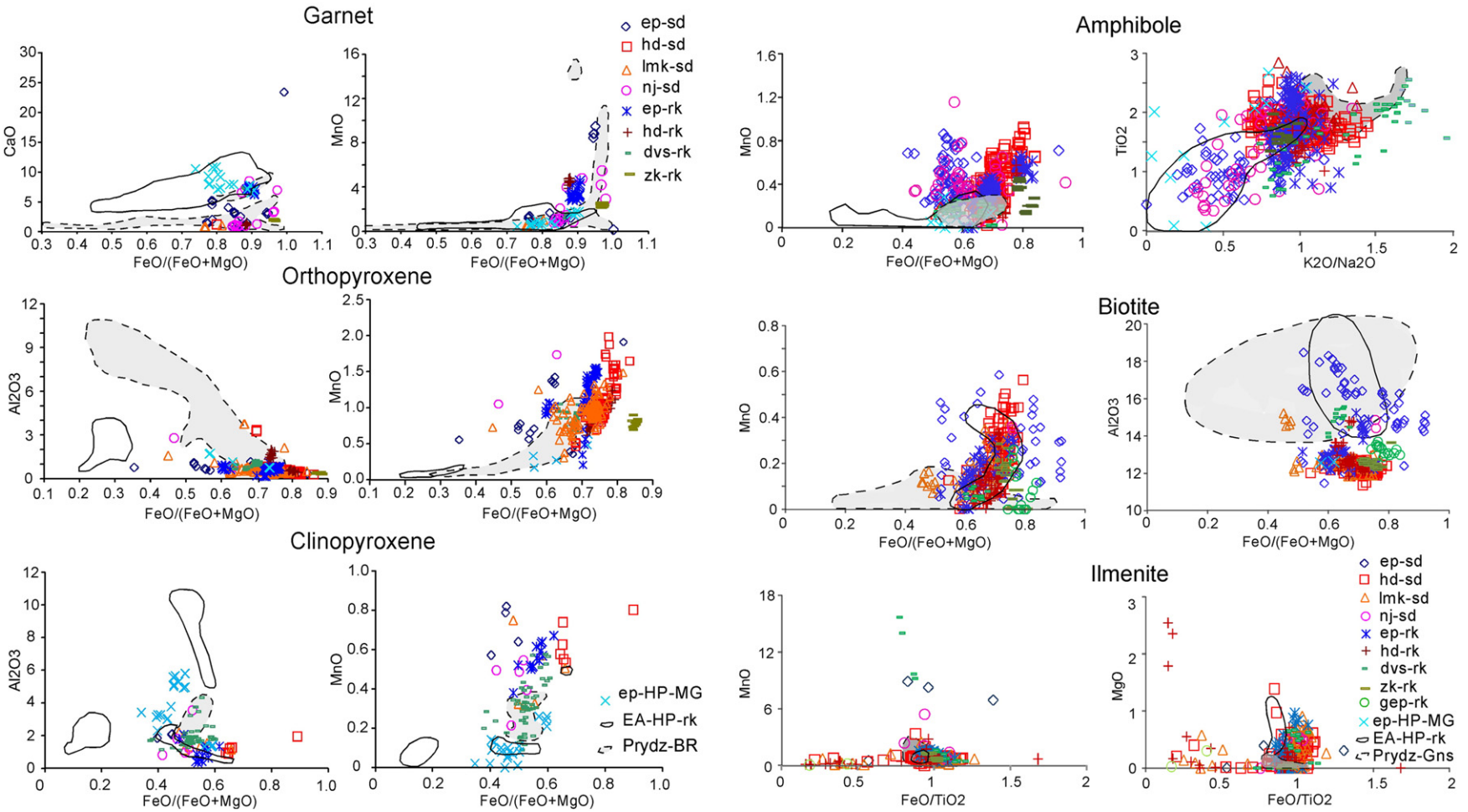

Fig. 6. EPMA mineral chemistry plots for garnet, orthopyroxene, clinopyroxene, amphibole, biotite and ilmenite. ep-sd: all microprobe data from four thin sections of different size portion from sample EP21-1; hd-sd: data from five thin sections of different size portion from sample HD17-1; lmk-sd: data from four thin sections from sample LMK23; nj-sd: data from three thin sections from NJ-02; ep-rk: data from six bedrock samples from south Gale Escarpment; hd-rk: data from six bedrock samples from Mount Harding; dvs-rk: data from six bedrock samples from Davis; gep-rk: data from two bedrock samples from north Gale Escarpment; zk-rk: data from two bedrock samples from Zakharroff Ridge; ep-HP-MG: data from high-pressure mafic granulites (Liu et al., 2009a); EP-HP-rk: this circled area is based on the mineral data from high grade metamorphic rocks (mainly eclogite) in East Antarctica; and Prydz-BR: the dash-line circled gray area is based on the mineral data from the basement rocks from Prydz Bay area.

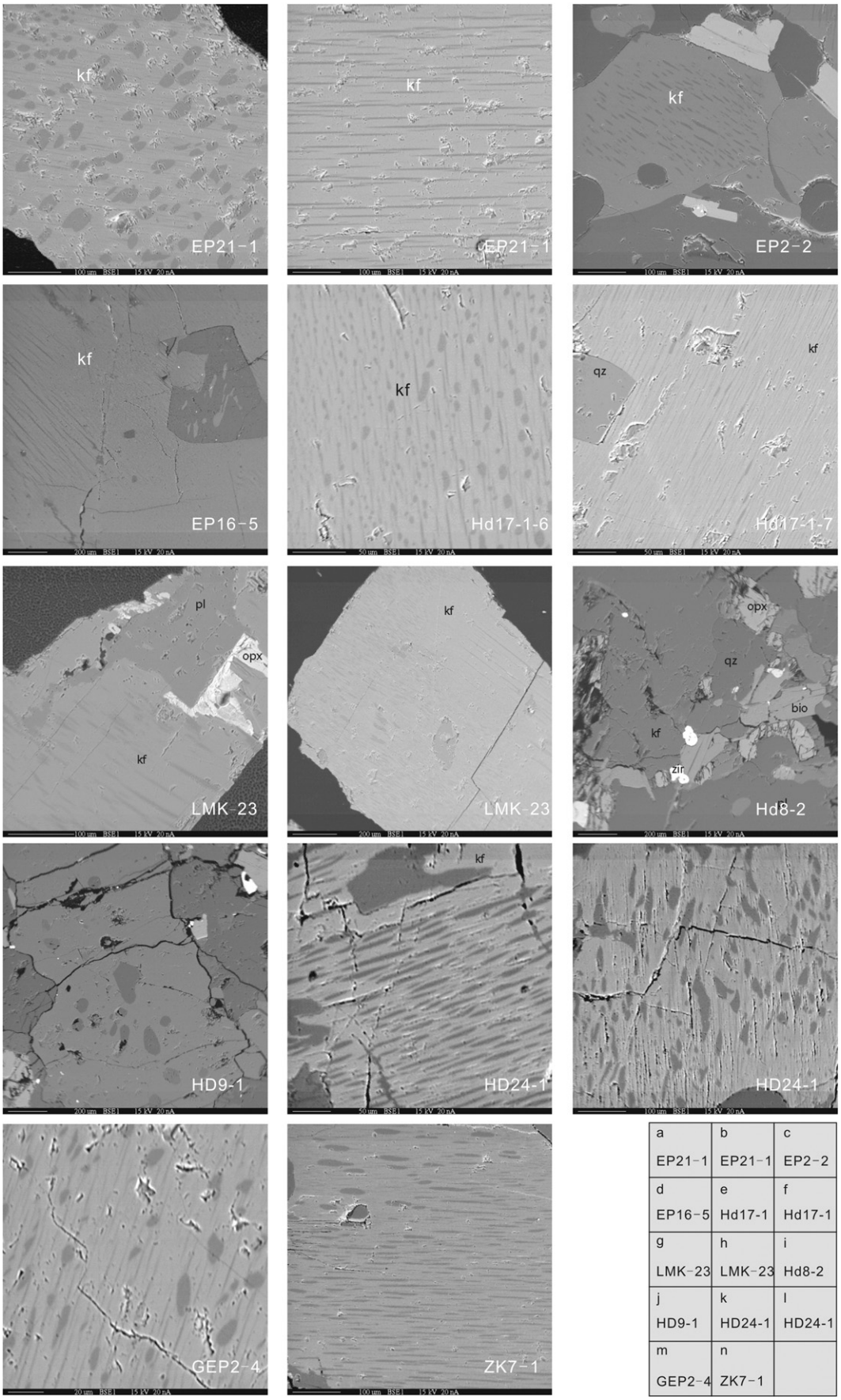

a EP21-1	b EP21-1	c EP2-2
d EP16-5	e Hd17-1	f Hd17-1
g LMK-23	h LMK-23	i Hd8-2
j HD9-1	k HD24-1	l HD24-1
m GEP2-4	n ZK7-1	

Fig. 7. K-feldspar perthitic texture from the detritus grains and bedrock from different locations. EP21-1, Hd17-1-6, Hd17-1-7, and LMK 23 are the K-feldspars from detrital grains; EP2-2, EP16-5, Hd8-2, HD9-1, HD24-1, GEP2-4, and ZK7-1 are the K-feldspars from bedrock.

Opx is common in the Grove Mountains area and they exist in both detritus and bedrock. Opx in the Grove Mountains, except EP detritus, is slightly more Fe and Mn rich than opx in the basement rocks from Prydz Bay area (Prydz-BR).

Cpx contents are low in both detritus and bedrock in the Grove Mountains. Cpx exists only in EP bedrock and not in HD rocks. But cpx is found in all detritus from each sampled location. The cpx from Prydz-BR was only reported from mafic granulites from McKaskle Hills (Liu et al., 2007b) and Grove Mountains (Liu et al., 2009a). Some cpx in the ep-HP-MG from Grove Mountains (Liu et al., 2009a) has similar chemistry to one group of EA-HP-rk.

The composition of amphibole and biotite in detritus from the Grove Mountains shows similarity to those in the bedrock but has wider compositional variation and HD detritus similar to the EP bedrock (Fig. 6b) indicating that the local exposed bedrock provided only part of the etritus minerals. Amphibole and biotite from the Grove Mountains contain higher FeO and MnO than amphibole and biotite from Prydz Bay and the Prince Charles Mountains (Fig. 6b); therefore, it is expected that the Grove Mountains rocks are slightly different in chemistry compared to Prydz Bay and Prince Charles Mountains rocks.

The following observations demonstrate that morainal detritus provides information about the composition of the local bedrock (around nunatak exposures and somewhat upstream): 1) the large detritus particles, like boulders and large pebbles, usually occur near their source; 2) HD loose detritus contains similar mineral assemblages as the HD tillite; and 3) the direction of glacier flow in Grove Mountains is from SEE to NWW (Cheng et al., 2007). The preserved glacial groves on the surface of bedrock at Gale Escarpment area indicate that the latest glacial maximum movement was 285–295°. 4) The west Mount Harding nunatak ridge is a large concave arête. The morainal belt begins at the base of this arête. This topographic relationship strongly suggests that the material in this morainal belt originates from Mount Harding nunatak itself. 5) The agreement between detrital zircon ages and the bedrock zircon ages imply that even though the morainal detritus might be sourced from a larger area than the local bedrock, the detritus should mainly record the composition of local bedrock. The 550–500 Ma tectonic activity had a strong impact on studied region. 6) The east side of Grove Mountains is an open Antarctic ice sheet and no exposed basement rocks can be detritus suppliers. The similarity between HD paleosol and EP detritus indicate the EP bedrock should have a wide distribution. 7) Based on the geomorphological character of these morainal belts, the source rock of these high-pressure mafic granulite pebbles should be to the northeast of Gale Escarpment nunatak ridge and the adjacent ice covered area.

5.2. Tectonothermal events at Grove Mountains

The geology and U–Pb zircon geochronology for the Grove Mountains area indicate: (1) the granite gneiss was originally intruded at 922 ± 32 Ma and was subjected to a metamorphic event at 529 ± 14 Ma (Zhao et al., 2000; Liu et al., 2007a). Whole-rock and mineral Sm–Nd isochron ages of 536 ± 3 Ma and 507 ± 30 Ma for granitic gneiss also suggest metamorphism at this time (Liu et al., 2013); (2) charnockite intrusion occurred at 547 ± 1 Ma (Liu et al., 2006); (3) charnockite vein intrusion at 535 ± 3 Ma, and granitic sills formed at 503 ± 2 Ma (Liu et al., 2006); and (4) mafic granulite formation at 850 °C and 0.61–0.67 GPa (Liu et al., 2003) at 529 ± 14 Ma (Zhao et al., 2000; Mikhalsky et al., 2001; Liu et al., 2009b).

In the Southern Prince Charles Mountains, previous geochronological studies have demonstrated that both the Rayner and Prydz orogenic events affected the region (Tingey, 1991; Boger et al., 2001, 2006; Mikhalsky et al., 2006; Phillips et al., 2007; Corvino et al., 2008). The 900–1000 Ma zircons in high-temperature metapelite, and the 530–490 Ma zircons in the numerous undeformed granites, the leucosome in high-strain zones, and the low Th/U zircon rims in 2120 Ma granitic gneiss indicate multiple tectonothermal overprints for the crustal terranes in this area (Boger et al., 2001, 2006; Phillips et al., 2006; Boger et al., 2008; Corvino et al., 2008). The Early Paleozoic reworking was regarded as the far-field stress associated with the final suturing of India to Antarctica (Corvino et al., 2008; Phillips et al., 2009). The multi-assembly model suggested that the Ediacaran–Cambrian orogeny (Kuunga Orogeny by Meert et al., 1995) developed along the margin of south-east Africa, southern India, southern Madagascar, east Australia, and East Antarctica (Meert et al., 1995; Meert and Van der Voo, 1997; Fitzsimons, 2000a; Boger et al., 2001; Meert, 2003; Zhao et al., 2003; Boger, 2011; Harley et al., 2013).

The detrital zircon results from our study show multiple peaks: 2400–2300 Ma, 900–800 Ma, and 550–450 Ma corresponding to the Mesoproterozoic, early Neoproterozoic, and Ediacaran–Cambrian tectonothermal events in Antarctic continent, respectively. Morainal detrital zircon ages are consistent with bedrock age patterns in the Grove Mountains and at Prydz Bay, although no Archean rocks have been found in the Grove Mountains area yet. There is a cluster of detrital zircon ages between 800 and 700 Ma. The discordant characters of these zircons indicate Pb loss. The projected arrays of these discordant ages point to 1000 Ma, implying that they are reworked zircons formed during Grenville event. During LA-ICP-MS analyses, the cores of zircon crystals were mainly analyzed to obtain the primary zircon growth period (Fig. 4). No traverse analyses were performed for most of the detrital zircons during this study. As a consequence, no age variation can be identified on the zoned zircons. In order to evaluate the potential Pb loss for the studied zircons, further work is needed.

The peaks on the age histograms of the detritus and tillite zircons (Fig. 5) are around 500 Ma. The detrital zircon ages for the paleosol sample also have a clear 500 Ma peak. Although, no HP mafic granulite lithic grains were found in detritus, some detrital garnet, opx, amphibole, and biotite show similar chemistry to those from the HP mafic granulite (Liu et al., 2009a). The mineral chemistry also suggests that the mafic minerals in Grove Mountains rocks have higher FeO and MnO compared with the Prydz Bay and Prince Charles Mountains area (Fig. 6a, b). These features indicate that some highly differentiated rocks should exist in the Grove Mountains but are not currently exposed. Accordingly, the 550–500 Ma tectonothermal activity in the Grove Mountains should correspond to the final amalgamation of East Antarctica.

6. Conclusions

Our detrital zircon and mineral chemistry study for the morainal belts has added new geochronological and geological constraints for the geologic evolution of the Grove Mountains area. The detrital zircon age distribution resembles the geochronology of the bedrock in the Grove Mountains. The glacial geomorphology and mineral chemistry suggest that the major sources for detritus should be close to the gravel belt. These observations provide strong support for the use of high-pressure mafic granulites from erratic boulders of glacial moraines as tectonic indicators in the Grove Mountains area. The high-pressure mafic granulites from morainal belts are evidence for the 550–500 Ma collisional event in the Prydz Belt (Liu et al., 2009a). Compared to data obtained from local bedrock, the detrital minerals show a broader compositional range and indicate more complex sources. Since a continental ice sheet covers Antarctica, the morainal detritus could carry more extensive geological information than bedrock exposures. Therefore, the morainal mineral study is a useful tool in Antarctica geological research in areas where very little bedrock is exposed.

Supplementary data to this article can be found online at http://dx.doi.org/10.1016/j.gr.2015.04.010.

Acknowledgments

We would like to thank Yitai Ju, Yangting Lin, Xiao Cheng, Feixin Huang, Aimin Fang, Wenjun Peng, Mingrong Pan, Xiaobo Liu, Jinyan Li and Xiaxing Xu for assistance during the fieldwork and Hujun Gong

for assistance with the LA-ICP-MS U–Pb zircon analyses. The fieldwork was completed during the 2005–2006 Chinese National Antarctic Research Expedition. Logistical and financial support by the Arctic and Antarctic Administration of China, the National Natural Science Foundation of China (No. 40872135), the Geological Investigation Project of the China Geological Survey (Nos. 12120113019000 and 1212010711509), and the Chinese Polar Environment Comprehensive investigation & Assessment Programmes (No. CHINARE2014-02-05) are gratefully acknowledged. Comments from anonymous reviewers provided additional concepts for the local geology and the style of presenting our data. Their contributions and proof reading from Eugene Smith and Dan Miggins have greatly improved this manuscript.

References

Andersen, T., 2002. Correction of common lead in U–Pb analyses that do not report ^{204}Pb. Chemical Geology 192, 59–79.

Bain, J.H.C., Harley, S.L., Seitz, H., Snape, I., Australian Geological Survey Organization, 2001. Geology of the Northern Vestfold Hills, East Antarctica. Bulletin. Royal Society of New Zealand 35.

Black, L.P., Williams, I.S., Compston, W., 1986. Four zircon ages from one rock: the history of a 3930 Ma-old granulite from Mount Sones, Enderby Land, Antarctica. Contributions to Mineralogy and Petrology 94, 427–437.

Black, L.P., Kinny, P.D., Sheraton, J.W., Delor, C.P., 1991. Rapid production and evolution of late Archaean felsic crust in the Vestfold Block of East Antarctica. Precambrian Research 50, 283–310.

Black, L.P., Sheraton, J.W., Tingey, R.J., Mcculloch, M.T., 1992. New U–Pb zircon ages from the Denman Glacier area, East Antarctica, and their significance for Gondwana reconstruction. Antarctic Science 4, 447–460.

Board, W.S., Frimmel, H.E., Armstrong, R.A., 2005. Pan-African tectonism in the western Maud Belt; P–T–t path for high-grade gneisses in the H.U. Sverdrupfjella, East Antarctica. Journal of Petrology 46 (4), 671–699.

Boger, S.D., 2011. Antarctica — before and after Gondwana. Gondwana Research 19, 335–371.

Boger, S.D., Miller, J.M., 2004. Terminal suturing of Gondwana and the onset of the Ross–Delamerian Orogeny: the cause and effect of an Early Cambrian reconfiguration of plate motions. Earth and Planetary Science Letters 219, 35–48.

Boger, S.D., White, R.W., 2003. The metamorphic evolution of metapelitic granulites from Radok Lake, northern Prince Charles Mountains, East Antarctica; evidence for an anticlockwise P/T path. Journal of Metamorphic Geology 21, 285–298.

Boger, S.D., White, R.W., 2005. Early Cambrian crustal shortening and a clockwise P–T–t path from the southern Prince Charles Mountains, East Antarctica: implications for the formation of Gondwana. Journal of Metamorphic Geology 23, 603–623.

Boger, S.D., Carson, C.J., Wilson, C.J.L., Fanning, C.M., 2000. Neoproterozoic deformation in the Radok Lake region of the northern Prince Charles Mountains, East Antarctica: evidence for a single protracted orogenic event. Precambrian Research 104, 1–24.

Boger, S.D., Wilson, C.J.L., Fanning, C.M., 2001. Early Paleozoic tectonism within the East Antarctic craton: the final suture between east and west Gondwana? Geology 29, 463–466.

Boger, S.D., Carson, C.J., Fanning, C.M., Hergt, J.M., Wilson, C.J.L., Woodhead, J.D., 2002. Pan-African intraplate deformation in the northern Prince Charles Mountains, East Antarctica. Earth and Planetary Science Letters 195, 195–210.

Boger, S.D., Wilson, C.J.L., Fanning, C.M., 2006. An Archaean province in the southern Prince Charles Mountains, East Antarctica: U–Pb zircon evidence for c. 3170 Ma granite plutonism and c. 2780 Ma partial melting and orogenesis. Precambrian Research 145, 207–228.

Boger, S.D., Maas, R., Fanning, C.M., 2008. Isotopic and geochemical constraints on the age and origin of granitoids from the central Mawson Escarpment, southern Prince Charles Mountains, East Antarctica. Contributions to Mineralogy and Petrology 155, 379–400.

Campbell, I.B., Claridge, G.G.C., 1987. Antarctica: Soils, Weathering Processes and Environment. Elsevier Science Publishers, Amsterdam (406 pp.).

Carson, C.J., Fanning, C.M., Wilson, C., 1996. Timing of the Progress Granite, Larsemann Hills: additional evidence for Early Palaeozoic orogenesis within the east Antarctic Shield and implications for Gondwana assembly. Australian Journal of Earth Sciences 43, 539–553.

Chen, T.Y., Xie, L.Z., Zhao, Y., Ren, L.D., Wang, Y.B., Yao, Y.P., 1995. Geological Map of the Antarctica (1:5000000). Geological Press, Beijing (In Chinese).

Cheng, X., Li, X.W., Shao, Y., Li, Z., 2007. DINSAR measurement of glacier motion in Antarctic Grove Mountain. Chinese Science Bulletin 52, 358–366.

Corvino, A.F., Boger, S.D., Henjes-Kunst, F., Wilson, C.J.L., Fitzsimons, I.C.W., 2008. Superimposed tectonic events at 2450 Ma, 2100 Ma, 900 Ma and 500 Ma in the North Mawson Escarpment, Antarctic Prince Charles Mountains. Precambrian Research 167, 281–302.

Daly, S.J., Fanning, C.M., Fairclough, M.C., 1998. Tectonic evolution and exploration potential of the Gawler Craton. AGSO Journal of Geology and Geophysics 17, 145–168.

Di Vincenzo, G., Palmeri, R., 2001. An ^{40}Ar/^{39}Ar investigation of high-pressure metamorphism and the retrogressive history of mafic eclogites from the Lanterman Range (Antarctica): evidence against a simple temperature control on argon transport in amphibole. Contributions to Mineralogy and Petrology 141, 15–35.

Di Vincenzo, G., Palmeri, R., Talarico, F., Andriessen, P.A.M., Ricci, C.A., 1997. Petrology and geochronology of eclogites from the Lanterman Range, Antarctica. Journal of Petrology 38 (10), 1391–1417.

Di Vincenzo, G., Talarico, F., Kleinschmidt, G., 2007. An 40Ar/39Ar investigation of the Mertz Glacier area (George V Land, Antarctica): implications for the Ross Orogen–East Antarctic Craton relationship and Gondwana reconstructions. Precambrian Research 152, 93–118.

Dirks, P.H.G.M., Wilson, C.J.L., 1995. Crustal evolution of the East Antarctic mobile belt in Prydz Bay: continental collision at 500 Ma? Precambrian Research 75, 189–207.

Elliot, D.H., Fanning, C.M., 2008. Detrital zircons from upper Permian and lower Triassic Victoria Group sandstones, Shackleton Glacier region, Antarctica: evidence for multiple sources along the Gondwana plate margin. Gondwana Research 13, 259–274.

Elliot, D.H., Fanning, C.M., Hulett, S.R.W., 2015. Age provinces in the Antarctic craton: evidence from detrital zircons in Permian strata from the Beardmore Glacier region, Antarctica. Gondwana Research 28 (1), 152–164. http://dx.doi.org/10.1016/j.gr.2014.03.013.

Fang, A.M., Liu, X.H., Lee, J.I., Li, X.L., Huang, F.X., 2004a. Sedimentary environments of the Cenozoic sedimentary debris found in the moraines of the Grove Mountains, East Antarctic and its climatic implications. Progress in Natural Science 14, 223–234.

Fang, A.M., Liu, X.H., Wang, W.M., Yu, L.J., Li, X.L., Huang, F.X., 2004b. Preliminary study on the spore-pollen assemblages found in Cenozoic sedimentary rocks in Grove Mountains, East Antarctica. Quaternary Sciences 24, 645–653.

Fanning, C.M., Dally, S.J., Bennett, V.C., Ménot, R.P., Peucat, J.J., Oliver, G.J.H., Monnier, O., 1995. The "Mawson Block": once contiguous Archaean to Proterozoic crust in the East Antarctic Shield and the Gawler Craton. In: Ricci, C.A. (Ed.), Abstracts, 7th International Symposium on Antarctic Earth Sciences, Sienna.

Fitzsimons, I., 2000a. A review of tectonic events in the East Antarctic Shield and their implications for Gondwana and earlier supercontinents. Journal of African Earth Sciences 31, 3–23.

Fitzsimons, I., 2000b. Grenville-age basement provinces in East Antarctica: evidence for three separate collisional orogens. Geology 28, 879–882.

Fitzsimons, I., 2003. Proterozoic basement provinces of southern and southwestern Australia, and their correlation with Antarctica. Special Publication. Geological Society of London 206, 93–130.

Fitzsimons, I., Harley, S.L., 1991. Geological relationships in high-grade gneiss of the Brattstrand Bluffs coastline, Prydz Bay, East Antarctica. Australian Journal of Earth Sciences 38, 497–519.

Fitzsimons, I., Kinny, P.D., Harley, S.L., 1997. Two stages of zircon and monazite growth in anatectic leucogneiss: SHRIMP constraints on the duration and intensity of Pan-African metamorphism in Prydz Bay, East Antarctica. Terra Nova 9, 47–51.

Flöttmann, T., Oliver, R.L., 1994. Review of Precambrian–Palaeozoic relationships at the craton margins of southeastern Australia and adjacent Antarctica. Precambrian Research 69, 293–306.

Fraser, G., McDougall, I., Ellis, D.J., Williams, I., 2000. Timing and rate of isothermal decompression in Pan-African granulites from Rundvågshetta, East Antarctica. Journal of Metamorphic Geology 18, 441–454.

Gao, S., Liu, X.M., Yuan, H.L., Hattendorf, B., Günther, D., Chen, L., Hu, S.H., 2002. Determination of forty-two major and trace elements of USGS and NIST SRM glasses by LA-ICPMS. Geostandards Newsletter 26, 181–196.

Godard, G., Palmeri, R., 2013. High-pressure metamorphism in Antarctica from the Proterozoic to the Cenozoic: a review and geodynamic implications. Gondwana Research 23, 844–864.

Goodge, J.W., Fanning, C.M., 2010. Composition and age of the East Antarctic Shield in eastern Wilkes Land determined by proxy from Oligocene–Pleistocene glaciomarine sediment and Beacon Supergroup sandstones, Antarctica. Geological Society of America Bulletin 122, 1135–1159.

Goodge, J.W., Williams, I.S., Myrow, P., 2004. Provenance of Neoproterozoic and lower Paleozoic siliciclastic rocks of the central Ross orogen, Antarctica: detrital record of rift-, passive-, and active-margin sedimentation. Geological Society of America Bulletin 116, 1253–1279.

Halpin, J.A., Daczko, N.R., Milan, L.A., Clarke, G.L., 2012. Decoding near-concordant U–Pb zircon ages spanning several hundred million years: recrystallisation, metamictisation or diffusion? Contributions to Mineralogy and Petrology 163, 67–85.

Hand, M., Kinny, P., 1996. SHRIMP Constraints on Palaeozoic High-T Exhumation in SW Prydz Bay, East Antarctica. pp. 61–62.

Harley, S.L., 1987. Precambrian geological relationships in high-grade gneisses of the Rauer Islands, East Antarctica. Australian Journal of Earth Sciences 34, 175–207.

Harley, S.L., 2003. Archaean–Cambrian crustal development of East Antarctica: metamorphic characteristics and tectonic implications. Geological Society, London, Special Publications 206, 203–230.

Harley, S.L., Black, L.P., 1997. A revised Archaean chronology for the Napier Complex, Enderby Land, from SHRIMP ion-microprobe studies. Antarctic Science 9, 74–91.

Harley, S.L., Snape, I., Black, L.P., 1998. The evolution of a layered metaigneous complex in the Rauer Group, East Antarctica: evidence for a distinct Archaean terrane. Precambrian Research 89, 175–205.

Harley, S.L., Fitzsimons, I.C.W., Zhao, Y., 2013. Antarctica and supercontinent evolution: historical perspectives, recent advances and unresolved issues. In: Harley, S.L., Fitzsimons, I.C.W., Zhao, Y. (Eds.), Antarctica and Supercontinent Evolution. Geological Society, London, Special Publications 383. http://dx.doi.org/10.1144/SP383.9.

Hensen, B.J., Zhou, B., 1995. A Pan-African granulite facies metamorphic episode in Prydz Bay, Antarctica: evidence from Sm–Nd garnet dating. Australian Journal of Earth Sciences 42, 249–258.

Hensen, B.J., Zhou, B., 1997. East Gondwana amalgamation by Pan-African collision? Evidence from Prydz Bay, East Antarctica. The Antarctic Region: Geological Evolution and Processespp. 115–119.

Hoffman, P.F., 1991. Did the breakout of Laurentia turn Gondwanaland inside-out? Science 252, 1409.
Hu, J.M., Liu, X.C., Zhao, Y., Xu, G., Ren, L.D., 2008. Advances in the study of the orogeny and structural deformation of Prydz Tectonic Belt in East Antarctica. Acta Geoscientica Sinica 29, 343–354.
Jacobs, J., Ahrendt, H., Kreutzer, H., Weber, K., 1995. K–Ar, ^{40}Ar–^{39}Ar and apatite fission-track evidence for Neoproterozoic and Mesozoic basement rejuvenation events in the Heimefrontfjella and Mannefallknausane (East Antarctica). Precambrian Research 75, 251–262.
Jamieson, S.S.R., Hulton, N.R.J., Sugden, D.E., Payne, A.J., Taylor, J., 2005. Cenozoic landscape evolution of the Lambert basin, East Antarctica: the relative role of rivers and ice sheets. Global and Planetary Change 45, 35–49.
Jenkins, C.J., Alibert, C., 1991. Sedimentary and metamorphic rock clasts from the Cenozoic diamictons of sites 739–743, Prydz Bay, East Antarctica. Proceeding of the Ocean Drilling Program, Scientific Results 119, 133–141.
Kelly, N.M., Harley, S.L., 2004. Orthopyroxene–corundum in Mg–Al-rich granulites from the Oygarden Islands, East Antarctica. Journal of Petrology 45, 1481–1512.
Kelsey, D.E., White, R.W., Powell, R., Wilson, C.J.L., Quinn, C.D., 2003a. New constraints on metamorphism in the Rauer Group, Prydz Bay, East Antarctica. Journal of Metamorphic Geology 21, 739–760.
Kelsey, D.E., Powell, R., Wilson, C., Steele, D., 2003b. (Th + U)–Pb monazite ages from Al–Mg-rich metapelites, Rauer Group, East Antarctica. Contributions to Mineralogy and Petrology 146, 326–340.
Kelsey, D.E., Hand, M., Clark, C., Wilson, C.J.L., 2007. On the application of in situ monazite chemical geochronology to constraining P–T–t histories in high-temperature (>850 Ma) polymetamorphic granulites from Prydz Bay, East Antarctica. Journal of the Geological Society 164, 667–683.
Kelsey, D.E., Wade, B.P., Collins, A.S., Hand, M., Sealing, C.R., Netting, A., 2008. Discovery of a Neoproterozoic basin in the Prydz Belt in East Antarctica and its implications for Gondwana assembly and ultrahigh temperature metamorphism. Precambrian Research 161, 355–388.
Kinny, P.D., 1998. Monazite U–Pb ages from east Antarctic granulites: comparisons with zircon U–Pb and garnet Sm–Nd ages. Geological Society of Australia 49, 250.
Kinny, P.D., Black, L.P., Sheraton, J.W., 1993. Zircon ages and the distribution of Archaean and Proterozoic rocks in the Rauer Islands. Antarctic Science 5, 193–206.
Kinny, P.D., Black, L.P., Sheraton, J.W., 1997. Zircon U–Pb ages and geochemistry of igneous and metamorphic rocks in the northern Prince Charles Mountains, Antarctica. Australian Geological Survey Organisation. Journal of Geology and Geophysics 16, 637–654.
Kröner, A., 1984. Late Precambrian plate tectonics and orogeny: a need to redefine the term Pan-African. In: Klerkx, J., Michot, J. (Eds.), African Geology. Tervuren Musee´ R. l'Afrique Centrale, Belgium, pp. 23–28.
Kröner, A., Stern, R.J., 2004. AFRICA|Pan-African orogeny. Encyclopedia of Geology 1, 1–12.
Lanyon, R., Black, L.P., Seitz, H., 1993. U–Pb zircon dating of mafic dykes and its application to the Proterozoic geological history of the Vestfold Hills, East Antarctica. Contributions to Mineralogy and Petrology 115, 184.
Li, X.L., Liu, X.H., Fang, A.M., Ju, Y.T., Yan, F.H., 2003a. Pliocene sporopollen in the Grove Mountains, East Antarctica. Marine Geology and Quaternary Geology 23, 35–39.
Li, X.L., Liu, X.H., Ju, Y.T., Huang, F.X., 2003b. Properties of soils in Grove Mountains, East Antarctica. Science in China Series D: Earth Sciences 46, 683–693.
Liu, X., Fang, A., Li, J., Hao, J., Yu, L., 2001. The first discovery of Cenozoic deposits in modern moraines of Grove Mountains, East Antarctica. Scientia Geologica Sinica 36.
Liu, X.C., Zhao, Y., Liu, X.H., 2002. Geological aspects of the Grove Mountains, East Antarctica. In: Gamble, J.A., Skinner, D.N.B., Henrys, S. (Eds.), Antarctica at the Close of a Millennium, pp. 161–166.
Liu, X.C., Zhao, Z.R., Zhao, Y., Chen, J., Liu, X.H., 2003. Pyroxene exsolution in mafic granulites from the Grove Mountains, East Antarctica: constraints on Pan-African metamorphic conditions. European Journal of Mineralogy 15, 55–65.
Liu, X.C., Jahn, B.M., Zhao, Y., Li, M., Li, H.M., Liu, X.H., 2006. Late Pan-African granitoids from the Grove Mountains, East Antarctica: age, origin and tectonic implications. Precambrian Research 145, 131–154.
Liu, X.C., Jahn, B.M., Zhao, Y., Zhao, G.C., Liu, X.H., 2007a. Geochemistry and geochronology of high-grade rocks from the Grove Mountains, East Antarctica: evidence for an Early Neoproterozoic basement metamorphosed during a single Late Neoproterozoic/Cambrian tectonic cycle. Precambrian Research 158, 93–118.
Liu, X.C., Zhao, Y., Zhao, G.C., Jian, P., Xu, G., 2007b. Petrology and geochronology of granulites from the McKaskle Hills, eastern Amery Ice Shelf, Antarctica, and implications for the evolution of the Prydz Belt. Journal of Petrology 48, 1443–1470.
Liu, X.C., Hu, J.M., Zhao, Y., Lou, Y.X., Wei, C.J., Liu, X.H., 2009a. Late Neoproterozoic/Cambrian high-pressure mafic granulites from the Grove Mountains, East Antarctica: PTt path, collisional orogeny and implications for assembly of East Gondwana. Precambrian Research 174 (1–2), 181–199.
Liu, X.C., Zhao, Y., Song, B., Liu, J., Cui, J.J., 2009b. SHRIMP U–Pb zircon geochronology of high-grade rocks and charnockites from the eastern Amery Ice Shelf and southwestern Prydz Bay, East Antarctica: constraints on Late Mesoproterozoic to Cambrian tectonothermal events related to supercontinent assembly. Gondwana Research 16, 342–361.
Liu, X.C., Zhao, Y., Hu, J.M., Liu, X.H., Qu, W., 2013. The Grove Mountains: a typical Pan-African metamorphic terrane in the Prydz belt, east Antarctica. Chinese Journal of Polar Research 25, 7–24 (In Chinese with English abstract).
Lovering, J.F., Travis, G.A., Comaford, D.J., Kelly, P.R., 1981. Evolution of the Gondwana Archaean Shield: zircon dating by ion-microprobe, and relationships between Australia and Wilkes Land (Antarctica). In: Glover, J.E., Groves, D.I. (Eds.), Archaean Geology: Geological Society of Australia Special Publication.
Ludwig, K.R., 1999. Isoplot/Ex(v. 2.06): a geological toolkit for Microsoft EXCEL. Berkeley Geochronology Center Special, Publication 1.
Meert, J.G., 2003. A synopsis of events related to the assembly of eastern Gondwana. Tectonophysics 362, 1–40.
Meert, J.G., 2014. Strange attractors, spiritual interlopers and lonely wanderers: the search for pre-Pangean supercontinents. Geoscience Frontiers 5, 155–166.
Meert, J.G., Lieberman, B.S., 2008. The Neoproterozoic assembly of Gondwana and its relationship to the Ediacaran–Cambrian Radiation. Gondwana Research 14, 5–21.
Meert, J.G., Van der Voo, R., 1997. The assembly of Gondwana 800–550 Ma. Journal of Geodynamics 23, 223–235.
Meert, J.G., Van der Voo, R., Ayub, S., 1995. Paleomagnetic investigation of the Neoproterozoic Gagwe lavas and Mbozi Complex, Tanzania and the assembly of Gondwana. Precambrian Research 74, 225–244.
Mikhalsky, E.V., Sheraton, J.W., Beliatsky, B.V., 2001. Preliminary U–Pb dating of Grove Mountains Rocks: implications for the Proterozoic to Early Palaeozoic tectonic evolution of the Lambert Glacier–Prydz Bay Area (East Antarctica). Terra Antarctica 8, 3–10.
Mikhalsky, E.V., Beliatsky, B.V., Sheraton, J.W., Roland, N.W., 2006. Two distinct Precambrian terranes in the Southern Prince Charles Mountains, East Antarctica: SHRIMP dating and geochemical constraints. Gondwana Research 9, 291–309.
Moores, E.M., 1991. Southwest US–East Antarctic (SWEAT) connection: a hypothesis. Geology 19, 425–428.
Motoyoshi, Y., Ishikawa, M., 1997. Metamorphic and structural evolution of granulites from Rundvågshetta, Lützow–Holm Bay, East Antarctica. In: Ricci, C.A. (Ed.), Antarctic Regions: Geological Evolution and Processes. Terra Antartica Publication, Siena, pp. 65–72.
Oliver, R.L., Fanning, C.M., 1997. Australia and Antarctica: precise correlation of Palaeoproterozoic terrains. In: Ricci, C.A. (Ed.), The Antarctic Region: Geological Evolution and Processes. Terra Antarctica Publications, Siena, pp. 163–172.
Oliver, R.L., Fanning, C.M., 2002. Proterozoic geology east and southeast of Commonwealth Bay, George V Land, Antarctica, and its relationship to that of adjacent Gondwana terranes. In: Gamble, J.A., Skinner, D.N.B., Henrys, S. (Eds.), Antarctica at the Close of the Millennium. Bulletin-Royal Society of New Zealand 35, pp. 51–58 (Wellington).
Oliver, R.L., James, P.R., Collerson, K.D., Ryan, A.B., 1982. Precambrian geologic relationships in the Vestfold Hills, Antarctica. In: Craddock, C. (Ed.), Antarctic Geoscience. University of Wisconsin Press, Madison, pp. 435–444.
Palmeri, R., Ghiribelli, B., Ranalli, G., Talarico, F., Ricci, C.-A., 2007. Ultrahigh-pressure metamorphism and exhumation of garnet-bearing ultramafic rocks from the Lanterman Range (northern Victoria Land, Antarctica). Journal of Metamorphic Geology 25 (2), 225–243.
Peacock, S.M., Goodge, G.W., 1995. Eclogite-facies metamorphism preserved in tectonic blocks from a lower crustal shear zone, central Transantarctic Mountains, Antarctica. Lithos 36, 1–13.
Paul, E., Stüwe, K., Teasdale, J., Worley, B., 1995. Structural and metamorphic geology of the Windmill Islands, East Antarctica: field evidence for repeated tectonothermal activity. Australian Journal of Earth Sciences 42, 453–469.
Peucat, J.J., Ménot, R.P., Monnier, O., Fanning, C.M., 1999. The Terra Adélie basement in the East-Antarctica Shield: geological and isotopic evidence for a major 1.7 Ga thermal event; comparison with the Gawler Craton in South Australia. Precambrian Research 94, 205–224.
Peucat, J.J., Capdevila, R., Fanning, C.M., Ménot, R.-P., Pécora, L., Testut, L., 2002. 1.6 Ga felsic volcanic blocks in the moraines of the Terre Adélie craton, Antarctica: comparisons with the Gawler Range volcanics, South Australia. Australian Journal of Earth Sciences 49, 831–845.
Phillips, G., Wilson, C.J.L., Campbell, I.A., Allen, C.M., 2006. U–Th–Pb detrital geochronology from the southern Prince Charles Mountains, East Antarctica: defining the Archaean to Neoproterozoic Ruker Province. Precambrian Research 148, 292–306.
Phillips, G., White, R.W., Wilson, C.J.L., 2007. On the roles of deformation and fluid during rejuvenation of a polymetamorphic terrane: inferences on the geodynamic evolution of the Ruker Province, East Antarctica. Journal of Metamorphic Geology 25, 855–871.
Phillips, G., Kelsey, D.E., Corvino, A.F., Dutch, R.A., 2009. Continental reworking during overprinting orogenic events, Southern Prince Charles Mountains, East Antarctica. Journal of Petrology 50, 2017–2041.
Powell, C. McA, Pisarevsky, S.A., 2002. Late Neoproterozoic assembly of East Gondwana. Geology 30, 3–6.
Rino, S., Kon, Y., Sato, W., Maruyama, S., Santosh, M., Zhao, D., 2008. The Grenvillian and Pan-African orogens: world's largest orogenies through geologic time, and their implications on the origin of superplume. Gondwana Research 14, 51–72.
Romer, T., Mezger, K., Schmädicke, E., 2009. Pan-African eclogite facies metamorphism of ultramafic rocks in the Shackleton Range, Antarctica. Journal of Metamorphic Geology 27, 335–347.
Santosh, M., Morimoto, T., Tsutsumi, Y., 2006. Geochronology of the khondalite belt of Trivandrum Block, southern India: electron probe ages and implications for Gondwana tectonics. Gondwana Research 9, 261–278.
Seitz, H.M., 1994. Estimation of emplacement pressure for 2350 Ma high-Mg tholeiite dykes, Vestfold Hills, Antarctica. European Journal of Mineralogy 6, 195–208.
Sheraton, J.W., Black, L.P., McCulloch, M.T., 1984. Regional geochemical and isotopic characteristics of high-grade metamorphics of the Prydz bay area: the extent of Proterozoic reworking of Archaean continental crust in East Antarctica. Precambrian Research 26, 169–198.
Sheraton, J.W., Tingey, R.J., Oliver, R.L., Black, L.P., 1995. Geology the Bunger Hills–Denman Glacier region, East Antarctica. Australian Geological Survey Organisation Bulletin 244 (124 pp.).
Shiraishi, K., Hiroi, Y., Ellis, D.J., Fanning, C.M., Motoyoshi, Y., Nakai, Y., 1992. The first report of a Cambrian orogenic belt in East Antarctica—an ion microprobe study of the Lützow–Holm complex. Recent Progress in Antarctic Earth Science. Terra Scientific Publishing Company, Tokyo, pp. 29–35.

Shiraishi, K., Ellis, D.J., Hiroi, Y., Fanning, C.M., Motoyoshi, Y., Nakai, Y., 1994. Cambrian orogenic belt in East Antarctica and Sri Lanka: implications for Gondwana assembly. Journal of Geology 102, 47–65.
Shiraishi, K., Hokada, T., Fanning, C.M., Misawa, K., Motoyoshi, Y., 2003. Timing of events in eastern Dronning Maud Land, East Antarctica. Polar Geoscience 16, 76–99.
Sims, J.P., Hand, M., Wilson, C., Fanning, C.M., 2001. Cambrian-aged (UHT) ultra-high temperature metamorphism in the Rauer Group, East Antarctica. Abstracts—Geological Society of Australia 64, 174–175.
Snape, I., Black, L.P., Harley, S.L., 1997. Refinement of the timing of magmatism, high-grade metamorphism and deformation in the Vestfold Hills, East Antarctica, from new SHRIMP U–Pb zircon geochronology. In: Ricci, C.A. (Ed.), The Antarctic Region: Geological Evolution and Processes. Terra Antarctic Publication, Siena, pp. 139–148.
Stern, R.J., 1994. Arc assembly and continental collision in the Neoproterozoic East African Orogen: implications for the consolidation of Gondwanaland. Annual Review of Earth and Planetary Sciences 22, 319–351.
Thost, D., Hensen, B.J., Motoyoshi, Y., 1994. The geology of a rapidly uplifted medium and low-pressure granulite facies terrane of Pan-African age: the Bolingen Islands, Prydz Bay, East Antarctica. Petrology 2, 293–316.
Tingey, R.J., 1982. The geologic evolution of the Prince Charles Mountains — an Antarctic Archaean cratonic block. In: Craddock, C. (Ed.), Antarctic Geoscience. University of Wisconsin Press, Madison, pp. 455–464.
Tingey, R.J., 1991. The regional geology of Archaean and Proterozoic rocks in Antarctica. In: Tingey, R.J. (Ed.), The Geology of Antarctica. Oxford University Press, Oxford, pp. 1–73.
Tong, L., Wilson, C.J.L., 2006. Tectonothermal evolution of the ultrahigh temperature metapelites in the Rauer Group, East Antarctica. Precambrian Research 149, 1–20.
Tong, L., Wilson, C., Liu, X., 2002. A high-grade event of ~1100 Ma preserved within the ~500 Ma Mobile Belt of the Larsemann Hills, East Antarctica: further evidence from ^{40}Ar–^{39}Ar dating. Terra Antarctica 9, 73–86.
Veevers, J.J., 2004. Gondwanaland from 650–500 Ma assembly through 320 Ma merger in Pangea to 185–100 Ma breakup: supercontinental tectonics via stratigraphy and radiometric dating. Earth-Science Reviews 68, 1–132.
Veevers, J.J., Saeed, A., 2008. Gamburtsev Subglacial Mountains provenance of Permian–Triassic sandstones in the Prince Charles Mountains and offshore Prydz Bay: integrated U–Pb and TDM ages and host-rock affinity from detrital zircons. Gondwana Research 14, 316–342.
Veevers, J.J., Saeed, A., 2011. Age and composition of Antarctic bedrock reflected by detrital zircons, erratics, and recycled microfossils in the Prydz Bay–Wilkes Land–Ross Sea–Marie Byrd Land sector (70°–240° E). Gondwana Research 20, 710–738.
Veevers, J.J., Saeed, A., 2013. Age and composition of Antarctic sub-glacial bedrock reflected by detrital zircons, erratics, and recycled microfossils in the Ellsworth Land–Antarctic Peninsula–Weddell Sea–Dronning Maud Land sector (240°E–0°–015°E). Gondwana Research 23, 296–332.
Veevers, J.J., Saeed, A., O'Brien, P.E., 2008. Provenance of the Gamburtsev Subglacial Mountains from U–Pb and Hf analysis of detrital zircons in Cretaceous to Quaternary sediments in Prydz Bay and beneath the Amery Ice Shelf. Sedimentary Geology 211, 12–32.
Wang, Y., Liu, D., Ren, L., Tang, S., 2003. Advances in SHRIMP geochronology and their constraints on understanding the tectonic evolution of Larsemann Hills, East Antarctica. 9th International Symposium on Antarctic Earth Sciences, Potsdam, Germany, pp. 334–335.
Wang, Y., Tong, L., Liu, D., 2007. Zircon U–Pb ages from an ultra-high temperature metapelite, Rauer Group, east Antarctica: implications for overprints by Grenvillian and Pan-African events. In: Cooper, A.K., Raymond, C.R., The 10th ISAES Editorial Team (Eds.), Antarctica: A Keystone in a Changing World — Online Proceedings of the 10th ISAES: USGS Open-File Report 2007-1047, Short Research Paper 023 http://dx.doi.org/10.3133/of2007-1047.srp023 (4 pp.).
Wang, Y., Liu, D., Chung, S.-L., Tong, L., Ren, L., 2008. SHRIMP zircon age constraints from the Larsemann Hills region, Prydz Bay, for a late Mesoproterozoic to Early Neoproterozoic tectono-thermal event in East Antarctica. American Journal of Science 308, 573–617.
White, R.W., Clarke, G.L., 1993. Timing of Proterozoic deformation and magmatism in a tectonically reworked orogen, Rayner Complex, Colbeck Archipelago, East Antarctica. Precambrian Research 63, 1–26.
Will, T.M., Zeh, A., Gerdes, A., Frimmel, H.E., Millar, I.L., Schmädicke, E., 2009. Palaeoproterozoic to Paleozoic magmatic and metamorphic events in the Shackleton Range, East Antarctica: constraints from zircon and monazite dating, and implications for the amalgamation of Gondwana. Gondwana Research 172, 25–45.
Will, T.M., Frimmel, H.E., Zeh, A., Le Roux, P., Schmädicke, E., 2010. Geochemical and isotopic constraints on the tectonic and crustal evolution of the Shackleton Range, East Antarctica, and correlation with other Gondwana crustal segments. Gondwana Research 180, 85–112.
Wilson, C.J.L., Quinn, C., Tong, L., Phillips, D., 2007. Early Palaeozoic intracratonic shears and post-tectonic cooling in the Rauer Group, Prydz Bay, East Antarctica constrained by $^{40}Ar/^{39}Ar$ thermochronology. Antarctic Science 19, 339–353.
Yuan, H.L., Gao, S., Liu, X.M., Li, H., Günther, D., Wu, F., 2004. Accurate U–Pb age and trace element determinations of zircon by laser ablation-inductively coupled plasma-mass spectrometry. Geostandards and Geoanalytical Research 28, 353–370.
Zhang, L., Tong, L., Liu, X.H., Scharer, U., 1996. Conventional U–Pb age of the high-grade metamorphic rocks in the Larsemann Hills, East Antarctica. In: Pang, Z., Zhang, J., Sun, J. (Eds.), Advances in Solid Earth Sciences. Science Press, Beijing, pp. 27–35.
Zhao, Y., Song, B., Wang, Y., Chen, T.Y., 1991. Geochronological study of the metamorphic and igneous rocks of the Larsemann Hills, East Antarctica. Proceedings of the 6th ISAES(Abstracts), Tokyo. National Institute for Polar Research, Japan, pp. 662–663.
Zhao, Y., Song, B., Wang, Y., Ren, L., Li, J., Chen, T., 1992. Geochronology of the late granite in the Larsemann Hills, East Antarctica. Recent Progress in Antarctic Earth Sciencepp. 155–161.
Zhao, Y., Song, B., Zhang, Z.Q., Fu, Y.L., Chen, T.Y., Wang, Y.B., Ren, L.D., Yao, Y.P., Li, J.L., Liu, X.H., 1993. Pan-Africa thermal events of the Larsemann Hills and near areas, East Antarctica. Sciences in China (Series B) 9, 1000–1008.
Zhao, Y., Liu, X.H., Song, B., Zhang, Z.Q., Li, J.L., Yao, Y.P., Wang, Y.B., 1995. Constraints on the stratigraphic age of metasedimentary rocks from the Larsemann Hills, East Antarctica: possible implications for Neoproterozoic tectonics. Precambrian Research 75, 175–188.
Zhao, J.X., Ellis, D.J., Kilpatrick, J.A., McCulloch, M.T., 1997. Geochemical and Sr–Nd isotopic study of charnockites and related rocks in the northern Prince Charles Mountains, East Antarctica: implications for charnockite petrogenesis and Proterozoic crustal evolution. Precambrian Research 81, 37–66.
Zhao, Y., Liu, X.H., Wang, S., Song, B., 1997. Syn- and post-tectonic cooling and exhumation in the Larsemann Hills, East Antarctica. Episodes 20, 122–127.
Zhao, Y., Liu, X.C., Fanning, C.M., Liu, X.H., 2000. The Grove Mountains, a segment of a Pan-African orogenic belt in East Antarctica. 31th International Geological Congress, Rio de Janeiro, Brazil.
Zhao, Y., Liu, X.H., Liu, B., Liu, S.L.D., Wang, Y.B., Liu, P., 2001. Pan-African events in Prydz Bay, East Antarctica and its inference on East Gondwana tectonics. Gondwana Research 4, 842.
Zhao, Y., Liu, X.H., Liu, X.C., Song, B., 2003. Pan-African events in Prydz Bay, east Antarctica, and their implications for east Gondwana tectonics. Geological Society, London, Special Publications 206, 231–245.
Ziemann, M.A., Forster, H., Harlov, D.E., Frei, D., 2005. Origin of fluorapatite–monazite assemblages in a metamorphosed, sillimanite-bearing pegmatoid, Reinbolt Hills, East Antarctica. European Journal of Mineralogy 17, 567–579.